AJRCMB Articles in Press. Published on 03-March-2017 as 10.1165/rcmb.2016-0217OC

A NOVEL ANTIFIBROTIC MECHANISM OF NINTEDANIB AND PIRFENIDONE: INHIBITION OF COLLAGEN FIBRIL ASSEMBLY

Larissa Knüppel[1], Yoshihiro Ishikawa[2], Michaela Aichler[3], Katharina Heinzelmann[1], Rudolf Hatz[4,5], Jürgen Behr[5,6], Axel Walch[3], Hans Peter Bächinger[2], Oliver Eickelberg[1,7] and Claudia A. Staab-Weijnitz[1*]

[1]Comprehensive Pneumology Center, Helmholtz-Zentrum München, Munich, Germany; Member of the German Center of Lung Research (DZL)

[2]Department of Biochemistry and Molecular Biology, Oregon Health & Science University, Portland, OR 97239, USA; Shriners Hospital for Children, Research Department, Portland, OR 97239, USA.

[3]Research Unit Analytical Pathology, Helmholtz-Zentrum München, Munich, Germany

[4]Thoraxchirurgisches Zentrum, Klinik für Allgemeine-, Viszeral-, Transplantations-, Gefäß- und Thoraxchirurgie, Klinikum Großhadern, Ludwig-Maximilians-Universität, Munich, Germany;

[5]Asklepios Fachkliniken München-Gauting, Munich, Germany;

[6]Medizinische Klinik und Poliklinik V, Klinikum der Ludwig-Maximilians-Universität, Munich, Germany; Member of the German Center of Lung Research (DZL)

[7]Pulmonary and Critical Care Medicine University, Colorado Anschutz Medical Campus, Denver, Colorado, United States of America

[*]To whom correspondence should be addressed: Claudia Staab-Weijnitz, Comprehensive Pneumology Center, Ludwig-Maximilians-Universität and Helmholtz Zentrum München, Max-Lebsche-Platz 31, 81377 München, Germany, Tel.: 0049(89)31874681; Fax: 0049(89)31874661; Email: staab-weijnitz@helmholtz-muenchen.de

Author contributions:

Conception and design: LK, YI, KH, RH, JB, AW, HPB, OE, CSW

Experimental work, analysis, and interpretation: LK, YI, MA, HPB, CSW

Drafting the manuscript and intellectual content: LK, YI, MA, HPB, OE, CSW

Sources of support: This work was supported by the Helmholtz Association, the German Center for Lung Research (DZL), and the Shriners Hospital for Children (#85100).

Running title: IPF drugs inhibit collagen fibril formation

Descriptor Number: 3.11 Pulmonary Fibrosis/Fibroblast Biology

Word count (main text): 4440

At a glance commentary:

Scientific Knowledge on the Subject: Accumulation of extracellular matrix, mainly collagen, is a main feature of idiopathic pulmonary fibrosis (IPF). Nintedanib and pirfenidone, two recently for IPF approved therapeutics, decelerate disease progression, but their antifibrotic mechanisms of action are incompletely understood.

What This Study Adds to the Field: This study provides the first evidence for inhibition of collagen fibril formation as a major mechanism of action for nintedanib and pirfenidone and puts forward extracellular collagen self-assembly as a druggable target in IPF.

This article has an online data supplement, which is accessible from this issue's table of content online at www.atsjournals.org.

AJRCMB Articles in Press. Published on 03-March-2017 as 10.1165/rcmb.2016-0217OC

ABSTRACT

Rationale: Idiopathic pulmonary fibrosis (IPF) is characterized by excessive deposition of extracellular matrix, in particular collagens. Two IPF therapeutics, nintedanib and pirfenidone, decelerate lung function decline, but their underlying mechanisms of action are poorly understood. In this study we sought to analyze their effects on collagen synthesis and maturation at important regulatory levels.

Methods: Primary human fibroblasts from IPF patients and healthy donors were treated with nintedanib (0.01-1.0μM) or pirfenidone (0.1-1.0mM) in absence or presence of TGF-β1. Effects on collagen, fibronectin, FKBP10, HSP47 expression and collagen I and III secretion were analyzed by qPCR and Western Blot. Appearance of collagen fibrils was monitored by scanning electron microscopy (SEM) and kinetics of collagen fibril assembly was assessed in a light scattering approach.

Results: In IPF fibroblasts, nintedanib reduced the expression of collagen I, V, fibronectin and FKBP10 and attenuated secretion of collagen I and III. Pirfenidone also downregulated collagen V, but otherwise showed fewer and less pronounced effects. By and large, effects were similar in donor fibroblasts. For both drugs, electron microscopy of IPF fibroblast cultures revealed fewer and thinner collagen fibrils compared with untreated controls. Finally, both drugs dose-dependently delayed fibril formation of purified collagen I.

Conclusions: Both drugs act on important regulatory levels in collagen synthesis and processing. Nintedanib was more effective in downregulating profibrotic gene expression and collagen secretion. Importantly, both drugs inhibited collagen I fibril formation and caused reduction and an altered appearance of collagen fibril bundles, representing a completely novel mechanism of action for both drugs.

Key words: Idiopathic pulmonary fibrosis, extra cellular matrix, nintedanib, pirfenidone

Abstract word count: 250

INTRODUCTION

Idiopathic pulmonary fibrosis (IPF) is a progressive and fatal interstitial lung disease with a median survival of 3-5 years after diagnosis (1). The underlying pathogenic processes are poorly understood, but the aberrant fibrotic response is likely initiated by repeated micro-injuries to the airway and alveolar epithelium (2). This leads to secretion of fibrotic mediators, including transforming growth factor β (TGF-β), which results in the accumulation of myofibroblasts in alveolar regions. Multiple progenitor cells may contribute to the myofibroblast population, but the most well-established source is the interstitial fibroblast (3). Myofibroblasts synthesize and deposit excessive amounts of extracellular matrix (ECM) proteins, such as collagen type I, III, V, or fibronectin (4). The resulting accumulation of ECM in the alveolar region is the ultimate pathological feature of lung fibrosis, leading to progressive lung function decline (5).

A recent study highlights that collagens are the main components of newly synthesized ECM in lung fibrosis (6) but large-scale quantitative proteome approaches have also demonstrated that the extracellular matrix composition (the matrisome) is far more complex than previously assumed (7). In addition, the complexity of collagen biosynthesis and maturation is rarely taken into account in mechanistic studies for the evaluation of anti-fibrotic strategies. Collagen modification and folding in the rough endoplasmic reticulum (rER) requires several enzymes and molecular chaperones essential for post-translational modifications (PTMs) and the processing of procollagen into triple helices, where one of the rate-limiting steps is the *cis-trans* isomerization of proline residues catalyzed by rER resident peptidyl prolyl isomerases (PPIases) (8). Collagen triple helix formation is followed by its secretion, extracellular fibril formation and fiber assembly (9). Two ER proteins participating in this multistep process are

AJRCMB Articles in Press. Published on 03-March-2017 as 10.1165/rcmb.2016-0217OC

the collagen chaperones FK506-binding protein 10 (FKBP10, also called FKBP65) and heat-shock protein 47 (HSP47, also called SerpinH1) (9). Notably, both FKBP10 and HSP47 are upregulated in bleomycin-induced lung fibrosis and in IPF (10, 11). Secretion of procollagen from HSP47-deficient fibroblasts is reduced compared with control cells (12) and similarly, knockdown of FKBP10 in IPF fibroblasts decreases collagen type I synthesis and secretion (10). In addition, PTMs like hydroxylation of lysyl or prolyl residues, or glycosylation of hydroxylysines are essential for proper stability, assembly and secretion of procollagen, as well as for the final supramolecular structure of these molecules (13). For example, hydroxylation of proline residues on position three (3-Hyp) might play a role in inter-triple-helical interactions and probably assists in the assembly of supramolecular collagen and lateral fibril growth (14, 15).

Nintedanib and pirfenidone were recently approved for IPF therapy, as both drugs have been shown to slow down disease progression as measured by reduced lung function decline. Despite their widespread application in IPF in recent time, their mechanisms of action are poorly understood and remain to be fully elucidated (16, 17). Nintedanib, originally developed as an anti-cancer drug, is a receptor tyrosine kinase (RTK) inhibitor of platelet-derived growth factor receptor, fibroblasts growth factor receptor, and vascular endothelial growth factor receptor, which all play an important role in the pathogenesis of IPF (5). Pirfenidone is an anti-fibrotic, anti-inflammatory and anti-oxidant compound with beneficial effects in lung, hepatic, kidney and cardiac fibrosis, but its direct targets are unknown (18, 19). Several studies have investigated the effects of either nintedanib or pirfenidone on collagen type I expression or secretion in several cell types (10, 20-26). No study to-date, however, directly compared both drugs on the multiple stages of intracellular collagen

synthesis and extracellular maturation in the relevant cell type, *i.e.* the primary human lung fibroblast.

Therefore, the aim of our study was to comprehensively assess and directly compare the effects of nintedanib and pirfenidone on the different steps of collagen synthesis and maturation in primary human lung fibroblasts (phLF) from IPF patients and healthy donors. We analyzed the expression of various collagens and the collagen chaperones FKBP10 and HSP47 as well as collagen secretion in IPF and healthy phLF. Additionally we examined the effects of both drugs on levels of selected post-translational modifications of collagen in IPF fibroblasts, and on collagen fibril formation.

AJRCMB Articles in Press. Published on 03-March-2017 as 10.1165/rcmb.2016-0217OC

MATERIALS AND METHODS

For more details on Material and Methods, please refer to the online supplement. Statistical analysis was performed in GraphPadPrism 7.02 (GraphPad Software, San Diego, CA, USA.)

MTT cytotoxicity assay

See the online supplement.

Human lung material and culture of phLF

Primary human lung fibroblasts, isolated from human lung explant material of IPF patients or healthy donors, were obtained from the BioArchive CPC-M for lung diseases at the Comprehensive Pneumology Center (CPC Munich, Germany). All participants gave written informed consent and the study was approved by the local ethics committee of the Ludwig-Maximilians University of Munich, Germany. Isolation of phLF was performed as described previously (10). For more details, see the online supplement.

Co-treatment of IPF and donor phLF with TGF-β1 and nintedanib or pirfenidone

Cells were seeded at a density of 20.000 – 25.000 cells/cm^2 followed by starvation for 24 h in starvation medium (DMEM/F12, 0.5% FBS, 0.1 mM 2-phospho-L-ascorbic acid). Subsequently, cells were treated with or without TGF-β1 (R&D Systems, Minneapolis, MN) (2 ng/mL) and with nintedanib (0.01 µM, 0.1 µM, 1.0 µM) or pirfenidone (100 µM, 500 µM, 1000 µM) (both Selleck, Houston, TX) for 48h in starvation medium. Nintedanib and pirfenidone were dissolved in DMSO. The final DMSO concentration in the medium was always 1%.

RNA isolation and Real-Time quantitative Reverse-Transcriptase PCR (qRT-PCR) Analysis

See the online supplement.

Protein Isolation and Western Blot Analysis

See the online supplement.

Quantification of secreted collagen

Collagen I and III were precipitated from cell culture supernatant of cultured IPF and donor phLF as described previously (10). For more details, see the online supplement.

Collagen precipitation and analysis of post-translational modifications (PTM)

See the online supplement.

Scanning electron microscopy (SEM) for assessment of fibrils in the ECM of phLFs

IPF phLF were grown on glass slides, treated with nintedanib (1 μM) or pirfenidone (1 mM) in combination with TGF-β1 (2 ng/mL) for 48h and fixed with paraformaldehyde and glutaraldehyde 3% each in 0,1% sodium cacodylate buffer pH 7.4 (Electron Microscopy Sciences, Munich, Germany). The specimens were dehydrated in gradual ethanol and dried by the critical-point method, using CO_2 as the transitional fluid (Polaron Critical Point Dryer CPC E3000; Quorum Technologies, Ringmer, UK). Specimens were sputter-coated with a thin layer of platinum by a sputtering device (Emitech K575; Quorum Technologies, Ringmer, UK) and observed by SEM (SEM, JSM 6300F; JEOL, Eching, Germany). Fibril thickness was assessed by measuring the diameter of the smallest unit of fiber forming fibrils,

AJRCMB Articles in Press. Published on 03-March-2017 as 10.1165/rcmb.2016-0217OC

using the length measurement tool of the open source software ImageJ 1.50i (W.S. Rasband, NIH, National Institutes of Health, Bethesda, MD).

Collagen I fibril formation assay

This assay was carried out essentially as described previously (27). For more details, see the online supplement.

RESULTS

The applied concentrations of nintedanib and pirfenidone were well tolerated by IPF phLF

For *in vitro* experiments, we selected a range of nintedanib and pirfenidone concentrations similar to published studies (20, 23, 25). Notably, for pirfenidone, in efforts to adhere to physiologically relevant concentrations, we used 1.0 mM as highest concentration, although others have used pirfenidone in concentrations up to 10 mM in similar experiments (21, 26, 28). Initially, we analyzed the effect of increasing doses of nintedanib (0.01-1 μM) and pirfenidone (0.1-1.0mM) on the viability of IPF fibroblasts in an MTT assay. The used concentrations of nintedanib and pirfenidone were well tolerated for the treatment period of 48h (Figure E1).

Nintedanib reduced the expression and secretion of ECM components more effectively than pirfenidone in phLF

Next, we assessed the effect of different concentrations of both drugs on the expression and secretion of collagen I (COL1A1), III (COL3A1), V (COL5A1), fibronectin (FN1), and PAI-1 in lysates and cell culture supernatants from primary human IPF and donor fibroblasts. Nintedanib consistently downregulated transcript and protein levels of basal and TGF-β1 induced collagen I in IPF phLF (Figure 1A, C, E, G). Pirfenidone only marginally reduced TGF-β1-induced COL1A1 transcripts (Figure 1A, C) and collagen I protein remained largely unchanged (Figure 1E, G). Similar tendencies were observed in phLF isolated from healthy donor lungs (Figure 1B, D, F), with the exception of COL1A1 transcript (Figure 1B) and

AJRCMB Articles in Press. Published on 03-March-2017 as 10.1165/rcmb.2016-0217OC

levels of basal secreted collagen I (Figure 1H), which both, in contrast to IPF, appeared unaffected by nintedanib in donor fibroblasts.

Similarly, expression of collagen III was consistently downregulated by nintedanib in IPF fibroblasts on transcript and protein level, while pirfenidone merely regulated COL3A1 transcripts, an effect which again did not translate to protein level (Figure 2A, C, E). Interestingly, in donor fibroblasts, nintedanib increased and pirfenidone decreased *COL3A1* transcription (Figure 2B, D), while the amount of secreted collagen III remained largely unchanged or even tended to anti-correlate with transcript levels (Figure 2F).

As to collagen V, TGF-β1-induced collagen V was significantly reduced in IPF fibroblasts by both drugs, an effect which was only partly captured at transcript level (Figure 3A, C, E); similar trends were observed in donor phLF (Figure 1E, F).

Expression of fibronectin 1 (*FN1*) was consistently decreased by nintedanib on transcript and protein level, both in IPF and donor fibroblasts (Figure E2). In contrast, pirfenidone reduced FN1 mRNA, but not protein levels in IPF fibroblasts (Figure E2A, C, E) and had no significant effect in donor phLF (Figure E2B, D, F). Interestingly, pirfenidone actually showed a trend to increase FN1 protein levels in both IPF and donor phLF (Figure E2E, F).

Expression of PAI-1, a classical TGF-β-induced gene, was significantly reduced by nintedanib in IPF and donor fibroblasts, with a more pronounced effect in absence of TGF-β1 (Figure E3). Pirfenidone did not affect *PAI-1* expression.

In summary, in comparison to nintedanib, pirfenidone showed fewer effects on collagen expression and secretion, *FN1* and *PAI-1* expression. Notably, exceeding the effective concentration of nintedanib at least 500 times, a concentration of 0.5 to 1.0 mM pirfenidone

was necessary to achieve significant effects, *e.g.* on collagen I, III, V, and *FN1* expression in TGF-β1-treated IPF fibroblasts (Figure 1A, 2A, 3E, Figure E2A).

Nintedanib, but not pirfenidone, reduces the expression of the collagen chaperone FKBP10 in IPF fibroblasts

Next, we investigated the effects of nintedanib and pirfenidone on expression of *FKBP10* and *HSP47*, two collagen I chaperones. Nintedanib moderately, but significantly, downregulated protein levels of FKBP10 in mock- as well as in TGF-β1-treated IPF fibroblasts (Figure 4E). This effect was visible on transcript level already for TGF-β-treated samples (Figure 4A, C). In contrast, pirfenidone did not influence *FKBP10* expression in IPF fibroblasts (Figure 4A, C, E). Interestingly, here clearly different results were obtained with donor fibroblasts, where nintedanib failed to regulate *FKBP10* expression, and pirfenidone downregulated FKBP10 transcript but upregulated FKBP10 protein levels (Figure 4B, D, F). Regarding expression of the major collagen I chaperone HSP47, neither drug reduced HSP47 protein levels in phLF (Figure 5E, F), even if both therapeutics decreased basal HSP47 mRNA (Figure 5A-D).

Selected posttranslational modifications of collagen I are not affected by nintedanib or pirfenidone

PTMs have a major impact on essential collagen properties like the three-dimensional structure, thermodynamic stability and biological functions (14, 15), but to date it has not been assessed whether anti-fibrotic drugs affect PTMs of collagen secreted by IPF fibroblasts. Here, we tested whether nintedanib and pirfenidone affected levels of selected PTMs of collagen I. More specifically, we compared levels of prolyl-3-hydroxylation of the A1 site (Pro-986) and the A3 site (Pro-707) of the collagen α1 chain (14), prolyl-3-hydroxylation of

AJRCMB Articles in Press. Published on 03-March-2017 as 10.1165/rcmb.2016-0217OC

the A3 site (Pro-707) of the collagen α2 chain and, finally, the glycosylation site of hydroxylysine (Lys-174) of collagen type I. Neither drug appeared to affect levels of the assessed PTMs (Figure E4).

Nintedanib and pirfenidone affect collagen fibril formation in IPF fibroblasts

SEM was used to assess number, morphology, and thickness of extracellular fibrils formed in cultures of TGF-β1-treated IPF fibroblasts in absence and presence of nintedanib or pirfenidone. Extracellular collagen fibers were identified as unbranched and dense bundles of thread-like looking twisted fibrils which were randomly oriented, of variable length, and with a diameter of maximally 1 μm (Figure 6A) (29). Cell cultures that had been treated with 1.0 μM nintedanib or 1.0 mM pirfenidone displayed a markedly reduced number of fibers and changes in overall fiber structure. In presence of both drugs, fibers were overall shorter, showed a more frayed appearance than in control samples, and fibril thickness was significantly reduced in nintedanib- and pirfenidone-treated samples compared to control fibrils (Figure 6B).

Nintedanib and pirfenidone inhibit spontaneous collagen I fibril formation

It seemed unlikely that the effects on collagen fibril formation observed by SEM could be accounted for by the effects of both drugs on collagen synthesis and secretion only, in particular for pirfenidone. Therefore, we investigated the direct effect of both drugs on spontaneous collagen I fibril formation in a light scattering approach. This assay is a well-established method to study the formation of collagen fibrils in a solution of purified soluble collagen I. It relies on the principle that collagen I, initially dissolved in dilute acid,

spontaneously forms fibrils upon neutralization in a self-driven process. The resulting fibrils are similar to those formed *in vivo* and the process can be visualized by dynamic light scattering at 313 nm (30, 31). We found that both therapeutics were able to considerably delay fibril formation of purified collagen I already at micromolar concentrations in a dose-dependent manner (Figure 7, Table 1).

AJRCMB Articles in Press. Published on 03-March-2017 as 10.1165/rcmb.2016-0217OC

Table 1: Nintedanib and pirfenidone increase halftime values for fibril formation (fibril formation$_{50}$) dose-dependently. Halftime values for fibril formation (fibril formation$_{50}$) are defined as the time at which the absorbance reaches half the value of the total absorbance change. Data are derived from graphs shown in Figure 7 and given as mean ± SD. Statistical analysis was performed on halftime values relative to DMSO control using One-Way ANOVA. n.d., not determined (n=2)

concentration of indicated drug [µM]	**Fibril formation50 [min]**	**p-value (comparison to DMSO control, OneWay ANOVA)**
0 (DMSO control)	49.6 ± 2.1	
Nintedanib		
0.5	55.6 ± 2.1	n.d.
1.0	59.1 ± 2.0	0.000218 (***)
Pirfenidone		
1.25	54.2 ± 4.7	0.133
2.5	57.3 ± 4.6	n.d.
10	61.6 ± 3.1	0.00165 (**)

DISCUSSION

In this study, we demonstrated that nintedanib and pirfenidone affect collagen synthesis and maturation on several regulatory levels, including inhibition of collagen gene expression, collagen secretion, and, most importantly, fibril formation. In terms of intracellular regulation of synthesis of ECM components and collagen secretion, nintedanib was clearly more effective, as it 1) exerted its effects at substantially lower concentrations (up to 1000-fold) than pirfenidone, 2) affected expression and secretion of more ECM and ECM-related genes, *i.e.* fibronectin, FKBP10 and collagen I, and 3) showed more consistent effects on transcript and protein levels. With few exceptions, these effects were mostly similar in IPF and donor fibroblasts. Importantly, both drugs strongly inhibited extracellular fibril formation, and assessment of spontaneous fibril assembly using purified collagen I indicated that both drugs directly inhibited this process with comparable efficiency.

Both nintedanib and pirfenidone inhibited TGF-β-induced transcription of *COL1A1*, *COL3A1* and *FN1*. In agreement, previous reports by others have shown that nintedanib and pirfenidone counteract TGF-β signaling and downregulate these TGF-β target genes (23, 24, 32). While pirfenidone only showed these effects in the presence of exogenously added TGF-β1, nintedanib also affected basal levels of *COL1A1* in IPF fibroblasts and also basal levels of another TGF-β target gene, *PAI-1*, in both IPF and donor fibroblasts (Figures 1A and E3). As the platelet-derived growth factor (PDGF) receptor and fibroblast growth factor (FGF) receptor are known targets of the RTK inhibitor nintedanib, this might reflect inhibition of autocrine PDGF or FGF signaling, which has been shown to regulate collagen gene expression (5, 33, 34) via both ERK and PI3K/Akt signaling pathways (35). In agreement,

AJRCMB Articles in Press. Published on 03-March-2017 as 10.1165/rcmb.2016-0217OC

phosphorylation of Akt was decreased in response to nintedanib in all of our experiments (Figure E5A, B). In contrast, phosphorylation of ERK was not consistently changed, neither in IPF nor in donor fibroblasts (Figure E5C, D). In light of the time point studied (48 h after treatment start), this argues for a stronger and more sustained inhibition of the PI3K/Akt signaling pathway by nintedanib in our studies. Inhibition of PDGFR signaling, however, cannot explain all of our *in vitro* results, as a previous study from our lab (34) found that siRNA-mediated downregulation of PDGFR-α actually drastically increased levels of collagen V in primary human lung fibroblasts, which is in contrast to what we observe in presence of nintedanib.

It is striking that many of the observed effects only translated to the protein level in presence of nintedanib, but not pirfenidone. For instance, both drugs inhibit TGF-β-induced *COL1A1*, *COL3A1*, and *FN1* transcription whereas levels of collagen I protein, secreted collagen III, and fibronectin protein were only reduced by nintedanib in IPF fibroblasts (Figures 1, 2, E2). These results suggest that post-transcriptional regulation mechanisms are affected differently by the drugs and highlight the importance of analysis at the protein level in this context. Nevertheless, other studies have reported effects of pirfenidone on collagen I and/or fibronectin protein levels in normal phLF (20, 26), alveolar epithelial cells (21), and nasal polyp fibroblasts (28). These discrepancies, however, may be the result of the use of substantially higher concentrations of pirfenidone in those studies (1.6 mM up to 10 mM). Notably, during standard treatment of IPF patients with pirfenidone (three daily doses of 801 mg pirfenidone), serum levels of pirfenidone do not exceed 100 μM (36), a concentration at which we did not observe any effect on phLF gene expression.

Both nintedanib and pirfenidone significantly downregulated collagen V in IPF fibroblasts and a similar trend was observed in donor fibroblasts (Figure 3E, F). Downregulation of collagen V levels in response to nintedanib or pirfenidone has, to our knowledge, not been reported before. Type V collagen is a minor component of collagen type I fibrils, which plays an important role in fibrogenesis and regulation of fiber size regulation (37-39). In IPF lungs, collagen V is heavily overexpressed compared to normal lungs (38). Importantly, in the context of the observed effects on fibril thickness (Figure 6B), collagen V has been shown to be crucial for initiation of collagen fibril assembly (39). Therefore, downregulation of collagen V by both drugs very likely contributes to the phenomenon of fewer and thinner fibrils in the extracellular space of primary human IPF fibroblasts described here (Figure 6). Interestingly, Hostettler *et al* (25) found that MMP2, an extracellular matrix metalloprotease which cleaves collagen V, is upregulated and its inhibitor, TIMP2, downregulated in response to nintedanib. This provides indirect evidence for increased extracellular degradation of collagen V, and, collectively, this suggests that nintedanib may decrease collagen V both via an intracellular and an extracellular mechanism.

To date, few studies have assessed the effects of nintedanib and pirfenidone on collagen secretion. Previously, we showed, using Sirius Red-based quantification of total collagen in cell culture supernatant, that nintedanib, but not pirfenidone, dose-dependently inhibited collagen secretion in IPF fibroblasts (10). Similarly, Hostettler *et al* reported a reduction of total secreted collagens in IPF and control fibroblasts upon nintedanib treatment (25). As collagen I and III are the most abundant fibrillar collagens in the lung interstitium and both are known to be increased in IPF (40), we further characterized inhibition of collagen secretion by both drugs looking at these two specific collagen subtypes in this study. Clearly,

AJRCMB Articles in Press. Published on 03-March-2017 as 10.1165/rcmb.2016-0217OC

nintedanib was more effective in inhibiting basal collagen I and TGF-β-induced collagen III secretion. Pirfenidone showed only weak inhibitory effects on basal collagen I secretion (Figure 1G), and, notably, no significant effects on collagen III secretion (Figure 2E). Given the observed inhibitory effect of nintedanib on total collagen secretion in our previous study (10), this suggests that nintedanib-induced downregulation of collagen III secretion contributes more strongly to the decrease of total secreted collagen than collagen I in IPF fibroblasts.

FKBP10 and HSP47 are rER-resident chaperones, critical for the proper folding of triple-helical procollagen (9, 12). Deficiency of both proteins leads to changes in the extracellular appearance of collagen fibrils as *e.g.* reduced collagen crosslinking (41, 42) or aberrant fibril formation (12). Both collagen chaperones are increased in animal models of bleomycin-induced lung fibrosis and in IPF patients (7, 10, 11) and we recently showed that siRNA-mediated downregulation of FKBP10 attenuates the expression and secretion of collagen in pHLF (10). Interestingly, it had been reported in two independent studies that pirfenidone downregulated expression of HSP47 in A549 cells and human lung fibroblasts, which suggested that pirfenidone exerted its anti-fibrotic effects in part via inhibition of intracellular collagen folding (21, 26). Therefore, we also assessed regulation of HSP47 and FKBP10 by nintedanib and pirfenidone in IPF and donor fibroblasts. Notably, nintedanib marginally, but significantly downregulated TGF-β-induced FKBP10 expression on transcript and protein level in IPF fibroblasts, while pirfenidone had no effect (Figure 4A, C, E). Strikingly, here a different pattern was observed for donor fibroblasts, where FKBP10 expression remained unaffected by nintedanib, but decreased at transcript and increased at protein level by pirfenidone (Figure 4B, D, F). Regarding HSP47 expression neither drug had an effect on

protein levels (4D), even if both drugs showed effects on transcript level (Figure 4E, F). Again, this is in contrast to previously reported results, but may be the result of higher pirfenidone concentrations used in these studies (21, 26).

Importantly, we found much fewer, thinner, and aberrantly structured collagen fibrils in the extracellular space of IPF fibroblasts treated with nintedanib or pirfenidone (Figure 6). This was particularly unexpected for pirfenidone, as we had only observed minor effects on collagen synthesis and secretion. As pointed out above, a partial explanation for this result may be the observed downregulation of type V collagen, which, even if it represents a minor constituent of collagen fibrils, appears to be crucial for collagen fibrogenesis (39). As deficiency of 3-Hyp has been shown to have major effects on lateral fibril growth (15), we also assessed hydroxylation of three 3-Hyp sites in collagen I, a comparatively rare collagen PTM, next to a lysyl glycosylation site in collagen I. However, we did not observe any effect of nintedanib or pirfenidone on these PTMs of collagen I (Figure E4). However, clearly there are many more collagen PTMs to consider and, in the light of the recently reported pro-fibrotic properties of ECM of IPF patients (43), a broader PTM fingerprinting of collagens in the context of fibrotic disease would undoubtedly be warranted.

Extracellular collagen fibril formation is mainly an entropy-driven self-assembly process (31). The so-called collagen D-stagger is formed by specific interactions of the residues along the triple-helical molecules with regularly staggered ends. After cleavage of the pro-peptides the collagen molecules become competent for fibril formation. We took advantage of the fact that this process can be studied in a straight-forward manner using purified pepsin-digested collagen (27) and found that low micromolar concentrations of both drugs inhibited collagen I

AJRCMB Articles in Press. Published on 03-March-2017 as 10.1165/rcmb.2016-0217OC

fibril formation with comparable efficiencies in a dose-dependent manner (Figure 7). Even if the exact molecular mechanisms remain obscure, it can be speculated that pirfenidone and nintedanib directly bind to collagen triple helices and mask or alter interaction sites due to changes in hydrophobicity or charges on the surface of the triple helix. Moreover, considering that higher concentrations of pirfenidone than of nintedanib were necessary to achieve the same amplitude of effect, nintedanib likely displays a stronger affinity to collagen than pirfenidone. Finally, as in our cell-free system pepsin-digested solubilized collagen is used, it can furthermore be concluded that the direct drug-collagen interaction takes place in the collagenous region of collagen and not within the telopeptides and propeptides which are typically removed by pepsin digestion.

Interestingly, inhibition of collagen I self-assembly has been proposed as a strategy for anti-fibrotic therapy, but this concept has received little attention in the field of lung fibrosis thus far (44). Instead, efforts have been undertaken to evaluate inhibition of collagen crosslinking by the enzyme lysyl oxidase-like 2 (LOXL2), notably a step subsequent to spontaneous fibril formation that stabilizes existing fibrils (31, 45). Very recently, however, a phase II study with a monoclonal anti-LOXL2 antibody has been terminated due to lack of efficacy (http://www.gilead.com/news/press-releases/2016/1/gilead-terminates-phase-2-study-of-simtuzumab-in-patients-with-idiopathic-pulmonary-fibrosis). Here we show, to our knowledge for the first time, that nintedanib and pirfenidone downregulate collagen V, a minor collagen important for initiation of extracellular fibrillogenesis, and also directly inhibit collagen fibril formation. This suggests that both therapeutics exert their anti-fibrotic actions at least in part via inhibition of collagen fibril formation, which provides additional support for the concept of inhibition of collagen self-assembly as a promising anti-fibrotic strategy.

This is a particularly interesting finding for pirfenidone, where the well-known anti-fibrotic effects *in vivo* to date stay in sharp contrast to concentrations in the millimolar range required to observe effects on fibrotic marker expression (19-21, 26, 36). Notably, our study is the first to offer evidence for an anti-fibrotic effect of pirfenidone *in vitro* which occurs at a micromolar concentration. For nintedanib, which affects the intracellular collagen pathway more strongly and in physiologically relevant concentrations, reduced fibril formation probably is a combined result of intracellular and extracellular events. Our findings furthermore emphasize that collagen V plays a hitherto underestimated role in fibrogenesis.

We observed only few differences between IPF and donor fibroblasts regarding effects of nintedanib and pirfenidone on expression of the studied targets. The most striking difference was observed for regulation of the collagen chaperone FKBP10, expression of which was consistently downregulated by nintedanib in IPF fibroblasts without evidence for downregulation in donor fibroblasts. Even more surprisingly, pirfenidone, which did not affect FKBP10 expression in IPF fibroblasts, decreased FKBP10 transcript and increased FKBP10 protein levels in donor fibroblasts. Another difference was that nintedanib had a stronger negative effect on *COL1A1*, *COL3A1* and *HSP47* transcription in IPF fibroblasts than in donor fibroblasts; at the same time, however, protein levels were unchanged or regulated similarly. Finally, both drugs downregulated basal collagen I secretion only in IPF fibroblasts and not in donor fibroblasts. Apart from those differences, by and large, tendencies of the effects of nintedanib and pirfenidone between IPF and donor fibroblasts on fibrotic markers, collagen chaperones and collagen secretion were similar. Notably, in a previous study, we also observed that effects on collagen synthesis and secretion were very similar in IPF and normal control fibroblasts and we ultimately pooled those results for data presentation (10).

AJRCMB Articles in Press. Published on 03-March-2017 as 10.1165/rcmb.2016-0217OC

This is also in agreement with two previously published studies (25, 46). Lehtonen *et al.* examined the effect of nintedanib and pirfenidone on fibroblast and myofibroblast properties and equally observed only marginal differences between cells from control and from IPF lungs. Hostettler *et al* studied collagen secretion by nintedanib in phLF and IPF fibroblasts and found that collagen secretion was downregulated to the same extent in both cell types.

In conclusion, our findings provide an overview and a direct comparison of the effects of the FDA/EMA-approved IPF drugs nintedanib and pirfenidone on different stages of expression and maturation of collagen in primary human lung fibroblast derived from IPF patients as well as from healthy donors. Nintedanib clearly was more efficient in inhibiting pro-fibrotic gene expression and collagen secretion than pirfenidone, both in terms of the required effective concentration as well as in number, consistency, and magnitude of its effects in independently derived IPF fibroblast lines. Finally, nintedanib and pirfenidone inhibited collagen fibril self-assembly, which represents a novel anti-fibrotic mechanism of action for both drugs. We suggest two independent potential mechanisms for this observation, namely downregulation of collagen V and inhibition of extracellular fibril formation by direct interaction of the drugs with triple-helical collagen.

ACKNOWLEDGMENTS

The authors thank Gabriele Mettenleiter and Elisabeth Hennen for excellent technical assistance as well as the CPC Research School and the HELENA graduate school.

REFERENCES

1. Kim DS, Collard HR, King TE, Jr. Classification and natural history of the idiopathic interstitial pneumonias. *Proc Am Thorac Soc* 2006; 3: 285-292.
2. Coward WR, Saini G, Jenkins G. The pathogenesis of idiopathic pulmonary fibrosis. *Ther Adv Respir Dis* 2010; 4: 367-388.
3. Rock JR, Barkauskas CE, Cronce MJ, Xue Y, Harris JR, Liang J, Noble PW, Hogan BL. Multiple stromal populations contribute to pulmonary fibrosis without evidence for epithelial to mesenchymal transition. *Proc Natl Acad Sci U S A* 2011; 108: E1475-1483.
4. Fernandez IE, Eickelberg O. The impact of TGF-beta on lung fibrosis: from targeting to biomarkers. *Proc Am Thorac Soc* 2012; 9: 111-116.
5. Wollin L, Wex E, Pautsch A, Schnapp G, Hostettler KE, Stowasser S, Kolb M. Mode of action of nintedanib in the treatment of idiopathic pulmonary fibrosis. *Eur Respir J* 2015; 45: 1434-1445.
6. Decaris ML, Gatmaitan M, FlorCruz S, Luo F, Li K, Holmes WE, Hellerstein MK, Turner SM, Emson CL. Proteomic analysis of altered extracellular matrix turnover in bleomycin-induced pulmonary fibrosis. *Mol Cell Proteomics* 2014; 13: 1741-1752.
7. Schiller HB, Fernandez IE, Burgstaller G, Schaab C, Scheltema RA, Schwarzmayr T, Strom TM, Eickelberg O, Mann M. Time- and compartment-resolved proteome profiling of the extracellular niche in lung injury and repair. *Mol Syst Biol* 2015; 11: 819.
8. Ishikawa Y, Bachinger HP. A molecular ensemble in the rER for procollagen maturation. *Biochim Biophys Acta* 2013; 1833: 2479-2491.
9. Ishikawa Y, Boudko S, Bachinger HP. Ziploc-ing the structure: Triple helix formation is coordinated by rough endoplasmic reticulum resident PPIases. *Biochim Biophys Acta* 2015; 1850: 1983-1993.
10. Staab-Weijnitz CA, Fernandez IE, Knüppel L, Maul J, Heinzelmann K, Juan-Guardela BM, Hennen E, Preissler G, Winter H, Neurohr C, Hatz R, Lindner M, Behr J, Kaminski N, Eickelberg O. FK506-Binding Protein 10, a Potential Novel Drug Target for Idiopathic Pulmonary Fibrosis. *Am J Respir Crit Care Med* 2015; 192: 455-467.
11. Razzaque MS, Nazneen A, Taguchi T. Immunolocalization of collagen and collagen-binding heat shock protein 47 in fibrotic lung diseases. *Mod Pathol* 1998; 11: 1183-1188.
12. Ishida Y, Kubota H, Yamamoto A, Kitamura A, Bachinger HP, Nagata K. Type I collagen in Hsp47-null cells is aggregated in endoplasmic reticulum and deficient in N-propeptide processing and fibrillogenesis. *Mol Biol Cell* 2006; 17: 2346-2355.
13. Hudson DM, Eyre DR. Collagen prolyl 3-hydroxylation: a major role for a minor post-translational modification? *Connect Tissue Res* 2013; 54: 245-251.
14. Weis MA, Hudson DM, Kim L, Scott M, Wu JJ, Eyre DR. Location of 3-hydroxyproline residues in collagen types I, II, III, and V/XI implies a role in fibril supramolecular assembly. *J Biol Chem* 2010; 285: 2580-2590.
15. Pokidysheva E, Zientek KD, Ishikawa Y, Mizuno K, Vranka JA, Montgomery NT, Keene DR, Kawaguchi T, Okuyama K, Bachinger HP. Posttranslational modifications in type

AJRCMB Articles in Press. Published on 03-March-2017 as 10.1165/rcmb.2016-0217OC

I collagen from different tissues extracted from wild type and prolyl 3-hydroxylase 1 null mice. *J Biol Chem* 2013; 288: 24742-24752.

16. Blackwell TS, Tager AM, Borok Z, Moore BB, Schwartz DA, Anstrom KJ, Bar-Joseph Z, Bitterman P, Blackburn MR, Bradford W, Brown KK, Chapman HA, Collard HR, Cosgrove GP, Deterding R, Doyle R, Flaherty KR, Garcia CK, Hagood JS, Henke CA, Herzog E, Hogaboam CM, Horowitz JC, King TE, Jr., Loyd JE, Lawson WE, Marsh CB, Noble PW, Noth I, Sheppard D, Olsson J, Ortiz LA, O'Riordan TG, Oury TD, Raghu G, Roman J, Sime PJ, Sisson TH, Tschumperlin D, Violette SM, Weaver TE, Wells RG, White ES, Kaminski N, Martinez FJ, Wynn TA, Thannickal VJ, Eu JP. Future directions in idiopathic pulmonary fibrosis research. An NHLBI workshop report. *Am J Respir Crit Care Med* 2014; 189: 214-222.
17. Richeldi L, du Bois RM, Raghu G, Azuma A, Brown KK, Costabel U, Cottin V, Flaherty KR, Hansell DM, Inoue Y, Kim DS, Kolb M, Nicholson AG, Noble PW, Selman M, Taniguchi H, Brun M, Le Maulf F, Girard M, Stowasser S, Schlenker-Herceg R, Disse B, Collard HR, Investigators IT. Efficacy and safety of nintedanib in idiopathic pulmonary fibrosis. *New Engl J Med* 2014; 370: 2071-2082.
18. Datta A, Scotton CJ, Chambers RC. Novel therapeutic approaches for pulmonary fibrosis. *Br J Pharmacol* 2011; 163: 141-172.
19. Schaefer CJ, Ruhrmund DW, Pan L, Seiwert SD, Kossen K. Antifibrotic activities of pirfenidone in animal models. *Eur Respir Rev* 2011; 20: 85-97.
20. Chambers RC, Mercer PF. Mechanisms of alveolar epithelial injury, repair, and fibrosis. *Ann Am Thorac Soc* 2015; 12 Suppl 1: S16-20.
21. Hisatomi K, Mukae H, Sakamoto N, Ishimatsu Y, Kakugawa T, Hara S, Fujita H, Nakamichi S, Oku H, Urata Y, Kubota H, Nagata K, Kohno S. Pirfenidone inhibits TGF-beta1-induced over-expression of collagen type I and heat shock protein 47 in A549 cells. *BMC Pulm Med* 2012; 12: 24.
22. Di Sario A, Bendia E, Svegliati Baroni G, Ridolfi F, Casini A, Ceni E, Saccomanno S, Marzioni M, Trozzi L, Sterpetti P, Taffetani S, Benedetti A. Effect of pirfenidone on rat hepatic stellate cell proliferation and collagen production. *J Hepatol* 2002; 37: 584-591.
23. Huang J, Beyer C, Palumbo-Zerr K, Zhang Y, Ramming A, Distler A, Gelse K, Distler O, Schett G, Wollin L, Distler JH. Nintedanib inhibits fibroblast activation and ameliorates fibrosis in preclinical models of systemic sclerosis. *Ann Rheum Dis* 2015.
24. Rangarajan S, Kurundkar A, Kurundkar D, Bernard K, Sanders YY, Ding Q, Antony VB, Zhang J, Zmijewski J, Thannickal VJ. Novel Mechanisms for the Anti-Fibrotic Action of Nintedanib. *Am J Respir Cell Mol Biol* 2015.
25. Hostettler KE, Zhong J, Papakonstantinou E, Karakiulakis G, Tamm M, Seidel P, Sun Q, Mandal J, Lardinois D, Lambers C, Roth M. Anti-fibrotic effects of nintedanib in lung fibroblasts derived from patients with idiopathic pulmonary fibrosis. *Respir Res* 2014; 15: 157.
26. Nakayama S, Mukae H, Sakamoto N, Kakugawa T, Yoshioka S, Soda H, Oku H, Urata Y, Kondo T, Kubota H, Nagata K, Kohno S. Pirfenidone inhibits the expression of HSP47 in TGF-beta1-stimulated human lung fibroblasts. *Life Sci* 2008; 82: 210-217.
27. Ishikawa Y, Bachinger HP. A substrate preference for the rough endoplasmic reticulum resident protein FKBP22 during collagen biosynthesis. *J Biol Chem* 2014; 289: 18189-18201.

28. Shin JM, Park JH, Park IH, Lee HM. Pirfenidone inhibits transforming growth factor beta1-induced extracellular matrix production in nasal polyp-derived fibroblasts. *Am J Rhinol Allergy* 2015; 29: 408-413.
29. Hashizume H, Hitomi J, Ushiki T. Growth of collagen fibrils produced by human osteosarcoma cells: high-resolution scanning electron microscopy. *Arch Histol Cytol* 1999; 62: 327-335.
30. Williams BR, Gelman RA, Poppke DC, Piez KA. Collagen fibril formation. Optimal in vitro conditions and preliminary kinetic results. *J Biol Chem* 1978; 253: 6578-6585.
31. Kadler KE, Holmes DF, Trotter JA, Chapman JA. Collagen fibril formation. *Biochem J* 1996; 316 (Pt 1): 1-11.
32. Lin X, Yu M, Wu K, Yuan H, Zhong H. Effects of pirfenidone on proliferation, migration, and collagen contraction of human Tenon's fibroblasts in vitro. *Invest Ophthalmol Vis Sci* 2009; 50: 3763-3770.
33. Pierce GF, Mustoe TA, Altrock BW, Deuel TF, Thomason A. Role of platelet-derived growth factor in wound healing. *J Cell Biochem* 1991; 45: 319-326.
34. Heinzelmann K, Noskovicova N, Merl-Pham J, Preissler G, Winter H, Lindner M, Hatz R, Hauck SM, Behr J, Eickelberg O. Surface proteome analysis identifies platelet derived growth factor receptor-alpha as a critical mediator of transforming growth factor-beta-induced collagen secretion. *Int J Biochem Cell Biol* 2016; 74: 44-59.
35. Tourkina E, Richard M, Gooz P, Bonner M, Pannu J, Harley R, Bernatchez PN, Sessa WC, Silver RM, Hoffman S. Antifibrotic properties of caveolin-1 scaffolding domain in vitro and in vivo. *Am J Physiol Lung Cell Mol Physiol* 2008; 294: L843-861.
36. Wollin L SJ, Ostermann A. The Effect Of Nintedanib Compared To Pirfenidone On Serum-Stimulated Proliferation Of Human Primary Lung Fibroblasts At Clinically Relevant Concentrations. *Am J Respir Crit Care Med* 2015; 191.
37. Parra ER, Teodoro WR, Velosa AP, de Oliveira CC, Yoshinari NH, Capelozzi VL. Interstitial and vascular type V collagen morphologic disorganization in usual interstitial pneumonia. *The journal of histochemistry and cytochemistry : official journal of the Histochemistry Society* 2006; 54: 1315-1325.
38. Vittal R, Mickler EA, Fisher AJ, Zhang C, Rothhaar K, Gu H, Brown KM, Emtiazdjoo A, Lott JM, Frye SB, Smith GN, Sandusky GE, Cummings OW, Wilkes DS. Type V collagen induced tolerance suppresses collagen deposition, TGF-beta and associated transcripts in pulmonary fibrosis. *PLoS One* 2013; 8: e76451.
39. Wenstrup RJ, Florer JB, Brunskill EW, Bell SM, Chervoneva I, Birk DE. Type V collagen controls the initiation of collagen fibril assembly. *J Biol Chem* 2004; 279: 53331-53337.
40. Dancer RC, Wood AM, Thickett DR. Metalloproteinases in idiopathic pulmonary fibrosis. *Eur Respir J* 2011; 38: 1461-1467.
41. Lindert U, Weis MA, Rai J, Seeliger F, Hausser I, Leeb T, Eyre D, Rohrbach M, Giunta C. Molecular Consequences of the SERPINH1/HSP47 Mutation in the Dachshund Natural Model of Osteogenesis Imperfecta. *J Biol Chem* 2015; 290: 17679-17689.
42. Barnes AM, Cabral WA, Weis M, Makareeva E, Mertz EL, Leikin S, Eyre D, Trujillo C, Marini JC. Absence of FKBP10 in recessive type XI osteogenesis imperfecta leads to diminished collagen cross-linking and reduced collagen deposition in extracellular matrix. *Hum Mutat* 2012; 33: 1589-1598.

AJRCMB Articles in Press. Published on 03-March-2017 as 10.1165/rcmb.2016-0217OC

43. Parker MW, Rossi D, Peterson M, Smith K, Sikstrom K, White ES, Connett JE, Henke CA, Larsson O, Bitterman PB. Fibrotic extracellular matrix activates a profibrotic positive feedback loop. *J Clin Invest* 2014; 124: 1622-1635.
44. Chung HJ, Steplewski A, Chung KY, Uitto J, Fertala A. Collagen fibril formation. A new target to limit fibrosis. *J Biol Chem* 2008; 283: 25879-25886.
45. Cox TR, Bird D, Baker AM, Barker HE, Ho MW, Lang G, Erler JT. LOX-mediated collagen crosslinking is responsible for fibrosis-enhanced metastasis. *Cancer Res Treat* 2013; 73: 1721-1732.
46. Lehtonen ST, Veijola A, Karvonen H, Lappi-Blanco E, Sormunen R, Korpela S, Zagai U, Skold MC, Kaarteenaho R. Pirfenidone and nintedanib modulate properties of fibroblasts and myofibroblasts in idiopathic pulmonary fibrosis. *Respir Res* 2016; 17: 14.

FIGURE LEGENDS

Figure 1: Nintedanib decreases collagen I expression and secretion more potently than pirfenidone in IPF fibroblasts

(**A-D**) Quantitative reverse transcriptase-polymerase chain reaction analysis of phLF isolated from (**A, C**)) IPF patients or (**B, D**) healthy donors treated for 48h with increasing concentrations of nintedanib (0.01, 0.1, 1 µM) or pirfenidone (100, 500, 1000 µM) in absence or presence of TGF-β1 (2 ng/mL). Transcript levels of COL1A1 are shown as -ΔCt values (**A, B**) as well as as transcript fold changes (**C, D**) to show the effect normalized to control. DEAH (Asp-Glu-Ala-His) Box Polypeptide 8 (DHX8) was used as endogenous control. Data are based on 7 (IPF) or 3 (donor) completely independent experiments and are given as mean ± SEM. Statistical significance between control and different concentrations of nintedanib or pirfenidone is indicated by horizontal brackets and asterisks for -ΔCt values and asterisks only for fold changes relative to 1.

(**E, F**) Western Blot analysis of phLF isolated from (**E**) IPF patients or (**F**) donors treated for 48h with increasing concentrations of nintedanib (0.01, 0.1, 1 µM) or pirfenidone (100, 500, 1000 µM) in absence or presence of TGF-β1 (2 ng/mL). Densitometric analysis and representative blots show the effect of nintedanib and pirfenidone on collagen I (Col I) protein expression relative to β-actin as loading control (ACTB). Data are based on 8 (IPF) or 3 (donor) completely independent experiments and are given as mean ± SEM. Statistical significance between control and different concentrations of nintedanib or pirfenidone is indicated by horizontal brackets and asterisks.

(**G, H**) Western Blot analysis of secreted collagen type I precipitated from cell culture supernatant of (**G**) IPF or (**H**) donor fibroblasts treated for 48h with increasing concentrations

AJRCMB Articles in Press. Published on 03-March-2017 as 10.1165/rcmb.2016-0217OC

of nintedanib (0.01, 0.1, 1.0 µM) or pirfenidone (100, 500, 1000 µM) in absence or presence of TGF-β1 (2ng/mL). Densitometric analysis and representative blots show the effects of nintedanib and pirfenidone on secreted collagen I after 48h. Data are based on 7 (IPF) or 3 (donor) completely independent experiments and are given as mean ± SEM. Statistical significance between control and different concentrations of nintedanib or pirfenidone is indicated by horizontal brackets and asterisks.

Statistical analysis was performed by One-Way ANOVA (post test: Bonferroni`s multiple comparison test:comparison against control). (*p<0.1, **p<0.01, ***p<0.001, ****p<0.0001). The well-known effect of TGF-β1 on these transcripts and proteins was significant, but is not specified in the interest of clarity. ctrl = control; TGF-β1 = transforming growth factor β1.

Figure 2: COL3A1 transcription is decreased by nintedanib in IPF fibroblasts and increased in donor fibroblasts, while collagen III secretion is decreased in both.

(**A-D**) Quantitative reverse transcriptase-polymerase chain reaction analysis of phLF isolated from (**A, C**) IPF patients or (**B, D**) healthy donors treated for 48h with increasing concentrations of nintedanib (0.01, 0.1, 1 µM) or pirfenidone (100, 500, 1000 µM) in absence or presence of TGF-β1 (2 ng/mL). Transcript levels of COL3A1 are shown as -ΔCt values (**A, B**) as well as as transcript fold changes (**C, D**) to show the effect normalized to control. DEAH (Asp-Glu-Ala-His) Box Polypeptide 8 (DHX8) was used as endogenous control. Data are based on 7 (IPF) or 3 (donor) completely independent experiments and are given as mean ± SEM. Statistical significance between control and different concentrations of nintedanib or pirfenidone is indicated by horizontal brackets and asterisks for -ΔCt values and asterisks only for fold changes relative to 1. The well-known effect of TGF-β1 on these

transcripts was significant, but is not specified in the interest of clarity. ctrl = control; TGF-β1 = transforming growth factor β1.

(**E, F**) Western Blot analysis of secreted collagen type III precipitated from cell culture supernatant of (**E**) IPF or (**F**) donor fibroblasts after treatment of phLF isolated from IPF patients treated for 48h with increasing concentrations of nintedanib (0.01, 0.1, 1.0 μM) or pirfenidone (100, 500, 1000 μM) in absence or presence of TGF-β1 (2ng/mL). Densitometric analysis and representative blots show the effects of nintedanib and pirfenidone on secreted collagen III after 48h. Data are based on 7 (IPF) or 3 (donor) completely independent experiments and are given as mean ± SEM. Statistical significance between control and different concentrations of nintedanib or pirfenidone is indicated by horizontal brackets and asterisks.

Statistical analysis was performed by One-Way ANOVA (post test: Bonferroni`s multiple comparison test: comparison against control). (*p<0.1, **p<0.01, ***p<0.001, ****p<0.0001).

Figure 3: Nintedanib and pirfenidone downregulate collagen V

(**A-D**) Quantitative reverse transcriptase-polymerase chain reaction analysis of phLF isolated from (**A, C**) IPF patients or (**B, D**) healthy donors treated for 48h with increasing concentrations of nintedanib (0.01, 0.1, 1 μM) or pirfenidone (100, 500, 1000 μM) in absence or presence of TGF-β1 (2 ng/mL). Transcript levels of (**A, C**) IPF and (**B, D**) donor phLF of *COL5A1* are shown as -ΔCt values (**A, B**) as well as as transcript fold changes (**C, D**) to show the effect normalized to control. DEAH (Asp-Glu-Ala-His) Box Polypeptide 8 (DHX8) was used as endogenous control. Data are based on 7 (IPF) or 3 (donor) completely independent

AJRCMB Articles in Press. Published on 03-March-2017 as 10.1165/rcmb.2016-0217OC

experiments and are given as mean ± SEM. Statistical significance between control and different concentrations of nintedanib or pirfenidone is indicated by horizontal brackets and asterisks for -ΔCt values and asterisks only for fold changes relative to 1.

(**E, F**) Western Blot analysis of phLF isolated from (**E**) IPF patients or (**F**) healthy donors treated for 48h with increasing concentrations of nintedanib (0.01, 0.1, 1 µM) or pirfenidone (100, 500, 1000 µM) in absence or presence of TGF-β1 (2 ng/mL). Densitometric analysis and representative blots show the effect of nintedanib and pirfenidone on Collagen V protein expression relative to β-actin (ACTB). Data are based on 8 (IPF) or 3 (donor) completely independent experiments and are given as mean ± SEM. Statistical significance between control and different concentrations of nintedanib or pirfenidone is indicated by horizontal brackets and asterisks.

Statistical analysis was performed by One-Way ANOVA (post test: Bonferroni`s multiple comparison test: comparison against control). (*p<0.1, **p<0.01, ***p<0.001, ****p<0.0001). The well-known effect of TGF-β1 on these transcripts and proteins was significant, but is not specified in the interest of clarity. ctrl = control; TGF-β1 = transforming growth factor β1.

Figure 4: Expression of the collagen chaperone FKBP10 is consistently downregulated by nintedanib in IPF, but more dynamically regulated by pirfenidone in donor fibroblasts

(**A-D**) Quantitative reverse transcriptase-polymerase chain reaction analysis of phLF isolated from (**A, C**) IPF patients or (**B, D**) healthy donors treated for 48h with increasing concentrations of nintedanib (0.01, 0.1, 1 µM) or pirfenidone (100, 500, 1000 µM) in absence

or presence of TGF-β1 (2 ng/mL). Transcript levels of (**A, C**) IPF and (**B, D**) donor phLF of *FKBP10* are shown as -ΔCt values (**A, B**) as well as as transcript fold changes (**C, D**) to show the effect normalized to control. DEAH (Asp-Glu-Ala-His) Box Polypeptide 8 (DHX8) was used as endogenous control. Data are based on 7 (IPF) or 3 (donor) completely independent experiments and are given as mean ± SEM. Statistical significance between control and different concentrations of nintedanib or pirfenidone is indicated by horizontal brackets and asterisks for -ΔCt values and asterisks only for fold changes relative to 1.

(**E, F**) Western Blot analysis of phLF isolated from (**E**) IPF patients or (**F**) healthy donors treated for 48h with increasing concentrations of nintedanib (0.01, 0.1, 1 μM) or pirfenidone (100, 500, 1000 μM) in absence or presence of TGF-β1 (2ng/mL). Densitometric analysis and representative blots show the effect of nintedanib and pirfenidone on FKBP10 protein expression relative to β-actin (ACTB). Data are based on 8 (IPF) or 3 (donor) completely independent experiments and are given as mean ± SEM. Statistical significance between control and different concentrations of nintedanib or pirfenidone is indicated by horizontal brackets and asterisks.

Statistical analysis was performed by One-Way ANOVA (post test: Bonferroni`s multiple comparison test: comparison against control). (*p<0.1, **p<0.01, ***p<0.001, ****p<0.0001). The well-known effect of TGF-β1 on these transcripts and proteins was significant, but is not specified in the interest of clarity. ctrl = control; TGF-β1 = transforming growth factor β1.

Figure 5: Expression of the major collagen I chaperone HSP47 is only reduced on transcript level by both drugs in IPF fibroblasts.

AJRCMB Articles in Press. Published on 03-March-2017 as 10.1165/rcmb.2016-0217OC

(**A-D**) Quantitative reverse transcriptase-polymerase chain reaction analysis of phLF isolated from (**A, C**) IPF patients or (**B, D**) healthy donors treated for 48h with increasing concentrations of nintedanib (0.01, 0.1, 1 µM) or pirfenidone (100, 500, 1000 µM) in absence or presence of TGF-β1 (2 ng/mL). Transcript levels of (**A, C**) IPF and (**B, D**) donor phLF of *HSP47* are shown as -ΔCt values (**A, B**) as well as transcript fold changes (**C, D**) to show the effect normalized to control. DEAH (Asp-Glu-Ala-His) Box Polypeptide 8 (DHX8) was used as endogenous control. Data are based on 7 (IPF) or 3 (donor) completely independent experiments and are given as mean ± SEM. Statistical significance between control and different concentrations of nintedanib or pirfenidone is indicated by horizontal bracketsand asterisks for -ΔCt values and asterisks only for fold changes relative to 1.

(**E, F**) Western Blot analysis of phLF isolated from (**E**) IPF patients or (**F**) healthy donors treated for 48h with increasing concentrations of nintedanib (0.01, 0.1, 1 µM) or pirfenidone (100, 500, 1000 µM) co-treated with or without TGF-β1 (2 ng/mL). Densitometric analysis and representative blots show the effect of nintedanib and pirfenidone on FKBP10 protein expression relative to β-actin (ACTB). Data are based on 8 (IPF) or 3 (donor) completely independent experiments and are given as mean ± SEM. Statistical significance between control and different concentrations of nintedanib or pirfenidone is indicated by horizontal brackets and asterisks.

Statistical analysis was performed by One-Way ANOVA (post test: Bonferroni`s multiple comparison test: comparison against control). (*p<0.1, **p<0.01, ***p<0.001, ****p<0.0001). The well-known effect of TGF-β1 on these transcripts and proteins was significant, but is not specified in the interest of clarity. ctrl = control; TGF-β1 = transforming growth factor β1.

Figure 6: Nintedanib and pirfenidone decrease number and thickness of collagen fibrils and alter their appearance.

(**A**) Scanning electron microscopy (SEM) of ECM fibrils deposited by phLF treated for 48h with nintedanib (1 µM, middle panel) or pirfenidone (1 mM, right panel) and TGF-β (2 ng/mL) showed fewer, thinner, and more frayed fiber bundles when compared to control (left panel). Magnification is indicated on the left side (upper panel: 250x; lower panel: 1000x). Results shown are representative images of 3 independent experiments with similar results.

(**B**) Thickness of single fibrils was measured in SEM pictures in three experiments using independently derived IPF fibroblasts (B). Statistical analysis was performed by a paired t-test. (**p<0.01).

Figure 7: Spontaneous collagen fibril formation is inhibited by both drugs in a dose-dependent manner

A collagen type I stock solution in 50 mM acetic acid was diluted to a final concentration of 0.1 µM into a 0.1 M $NaHCO_3$ buffer (pH 7.8) containing 0.15 M NaCl and 1 mM $CaCl_2$ and heated up to 34°C, followed by monitoring of absorbance (light scattering) at 313 nm. (**A**) Nintedanib (red, 0.5 µM, n=2; blue, 1.0 µM , n=5) and (**B**) pirfenidone (red, 1.25 µM, n=3; blue, 2.50 µM , n=2; green, 10.0 µM, n=3) on collagen type I fibril formation in comparison to DMSO control (black, n=4) are shown. The resulting halftime values for fibril formation are given in Table 1.

Figure 1

AJRCMB Articles in Press. Published on 03-March-2017 as 10.1165/rcmb.2016-0217OC

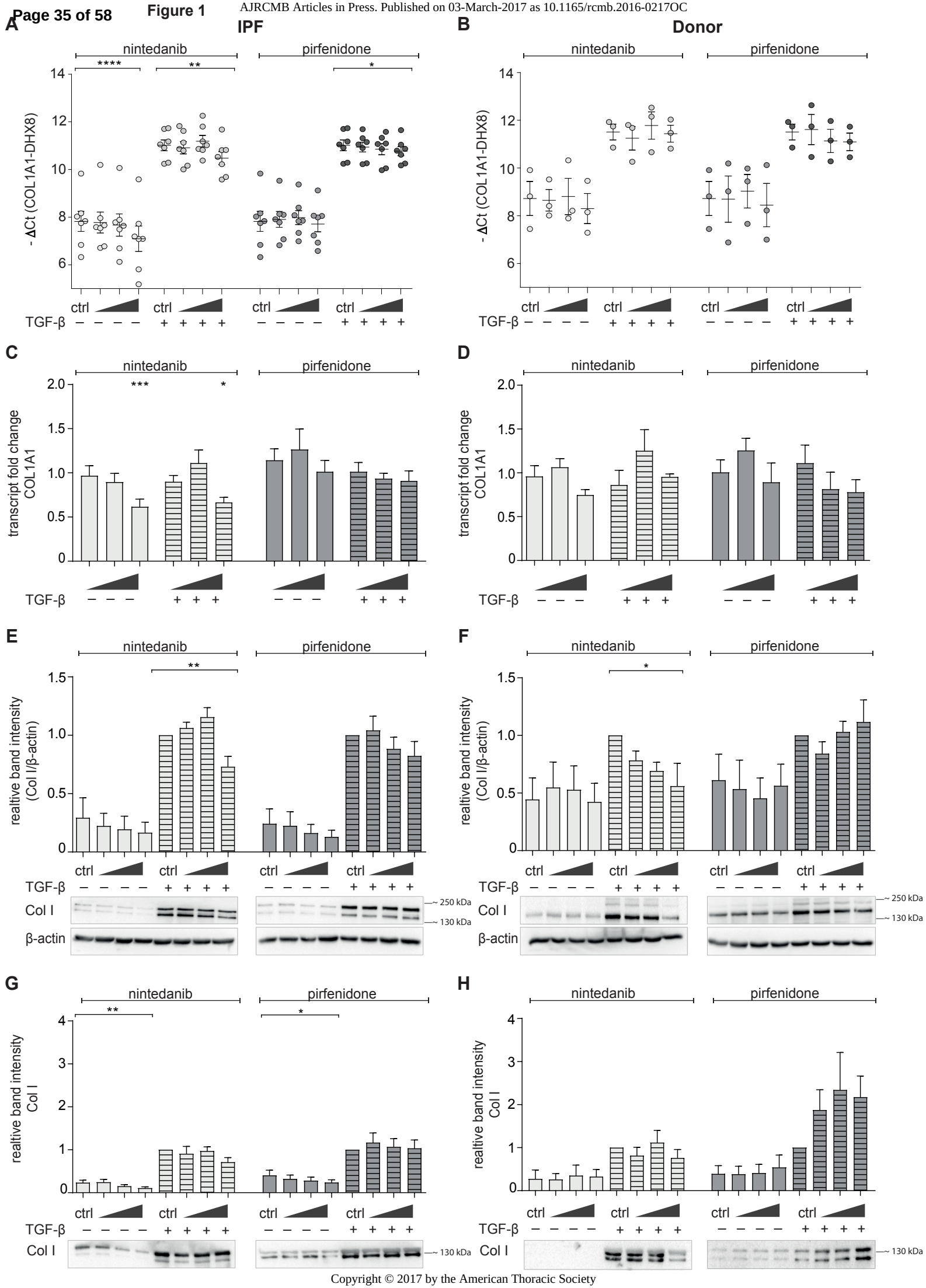

Figure 2

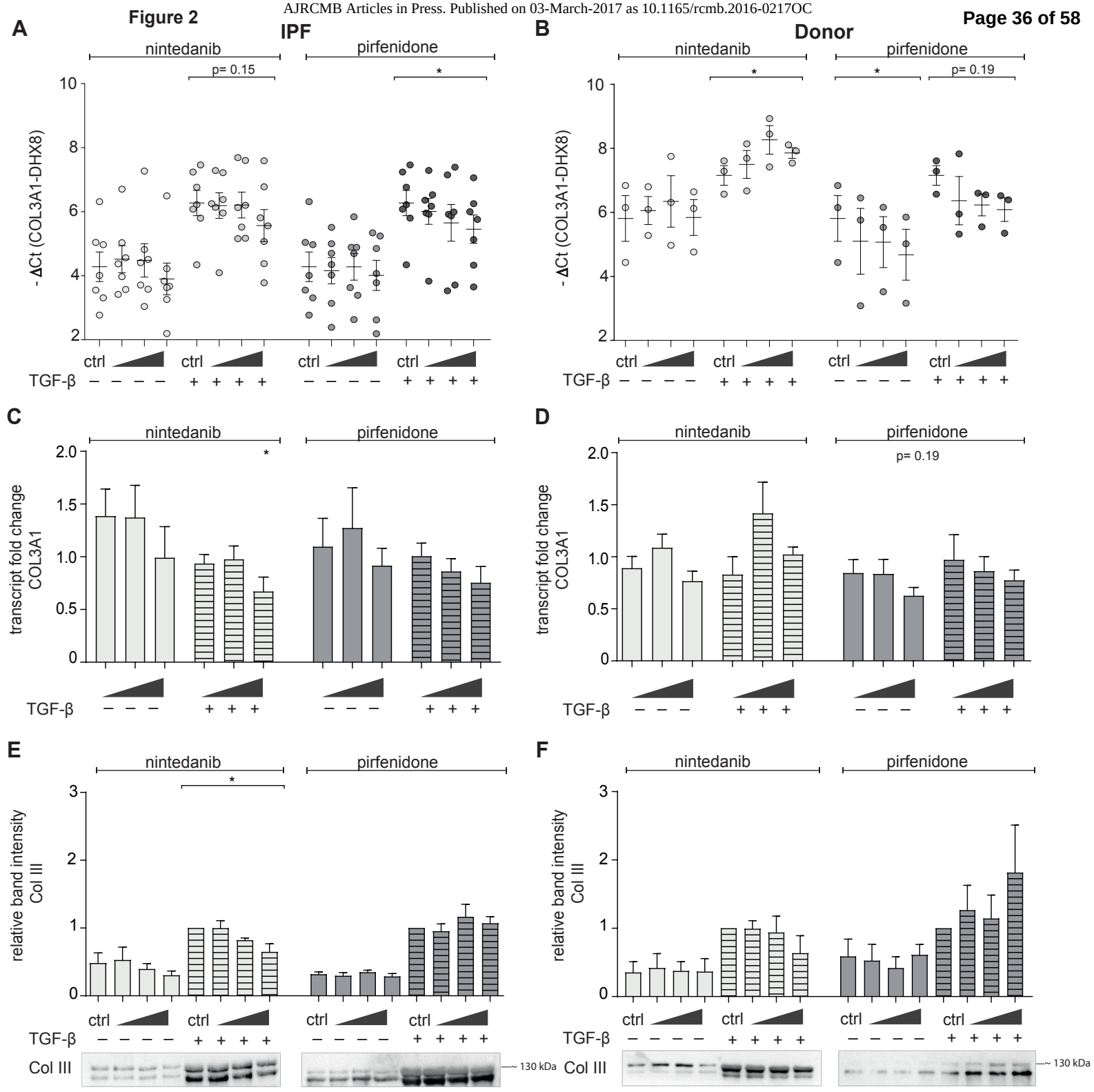

Figure 3

AJRCMB Articles in Press. Published on 03-March-2017 as 10.1165/rcmb.2016-0217OC

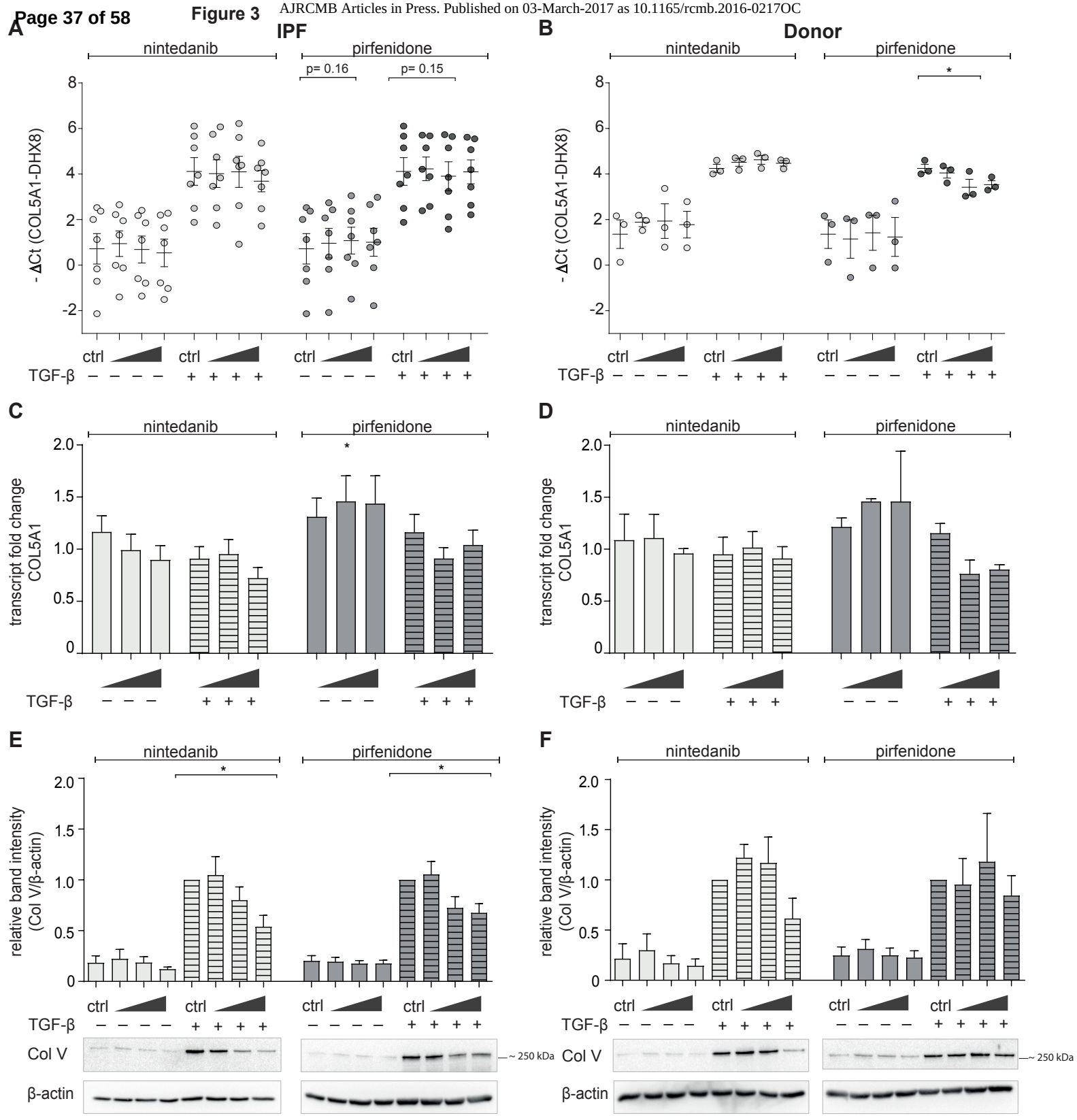

AJRCMB Articles in Press. Published on 03-March-2017 as 10.1165/rcmb.2016-0217OC

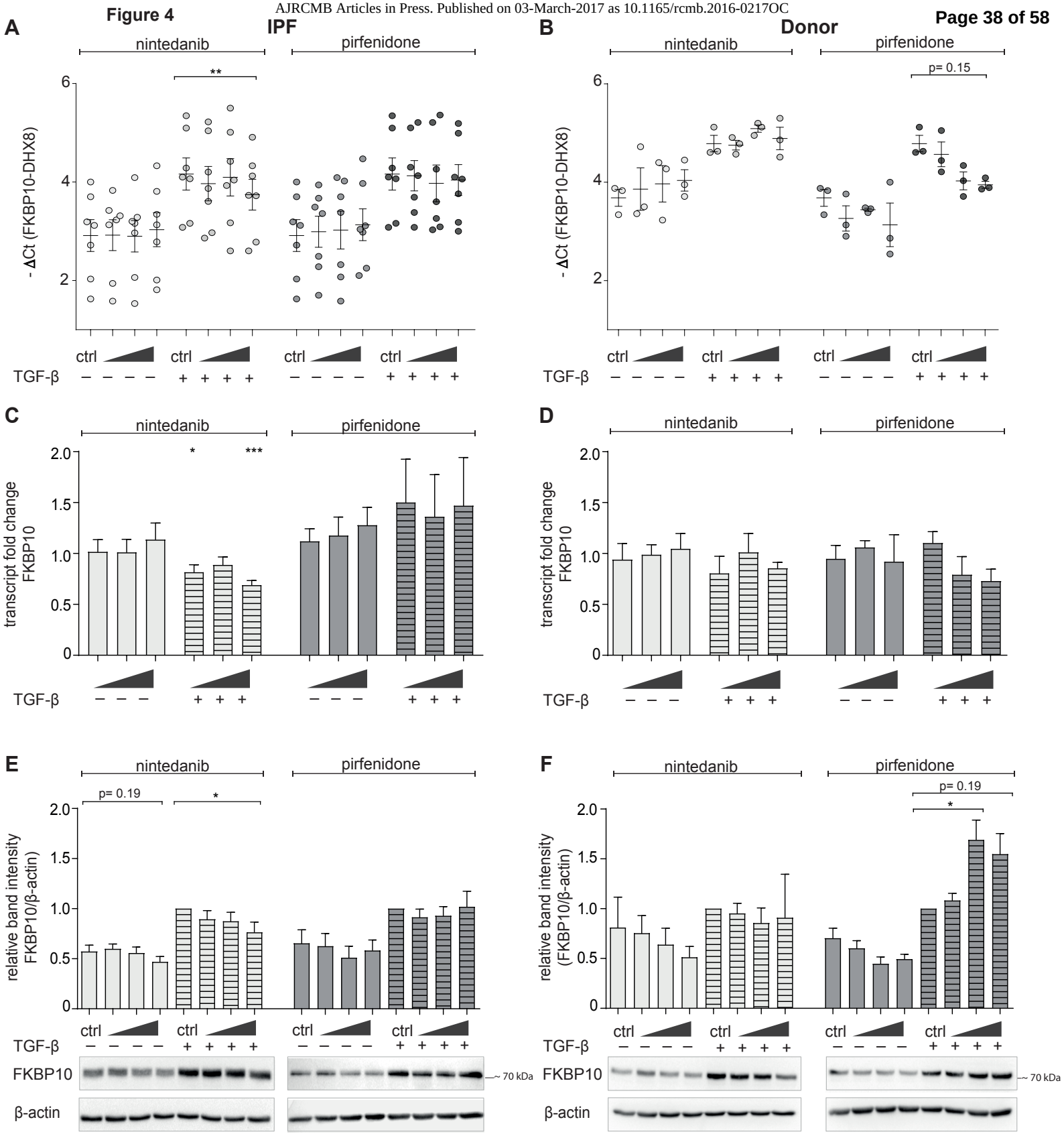

Figure 5

AJRCMB Articles in Press. Published on 03-March-2017 as 10.1165/rcmb.2016-0217OC

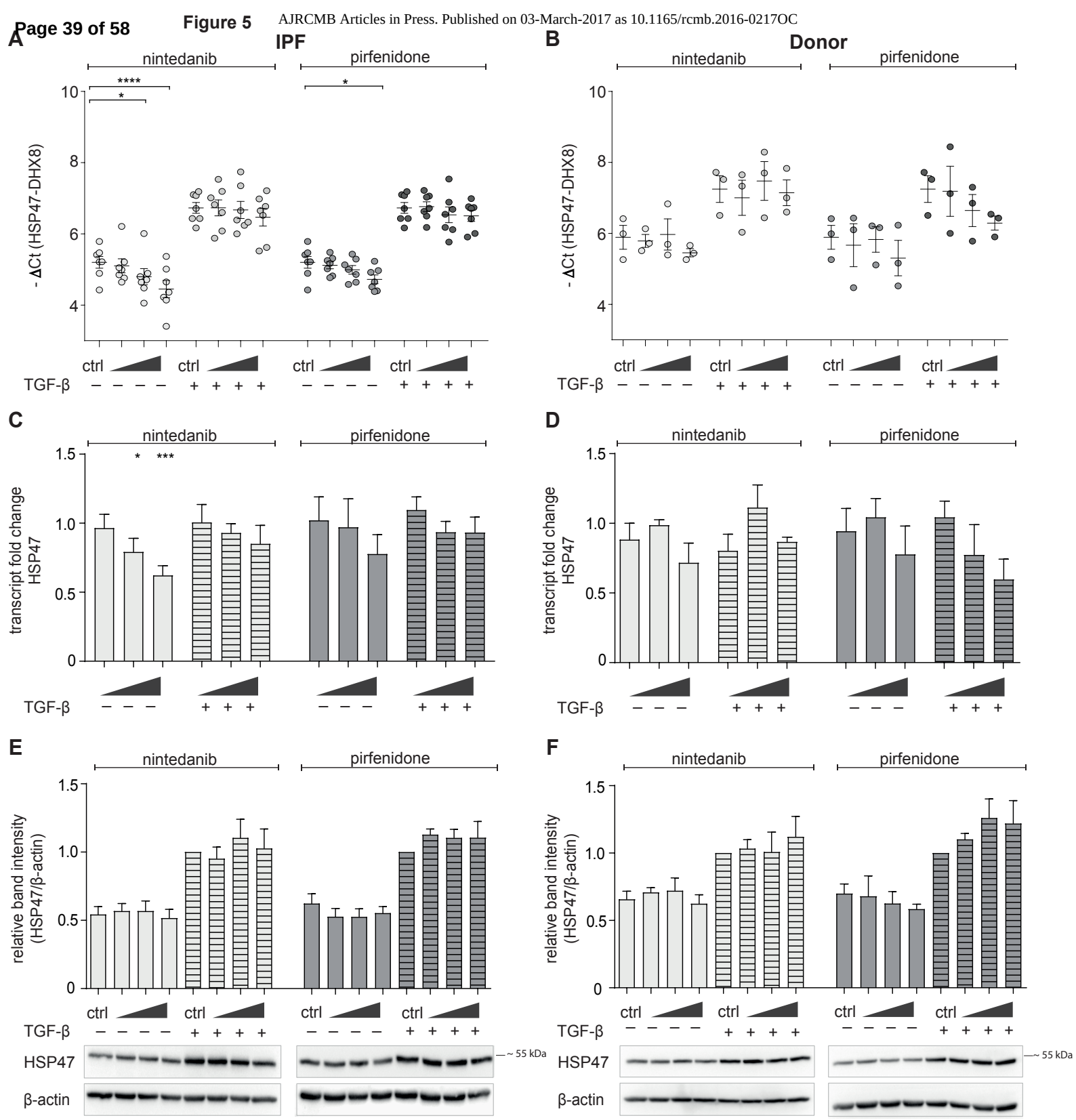

AJRCMB Articles in Press. Published on 03-March-2017 as 10.1165/rcmb.2016-0217OC

A

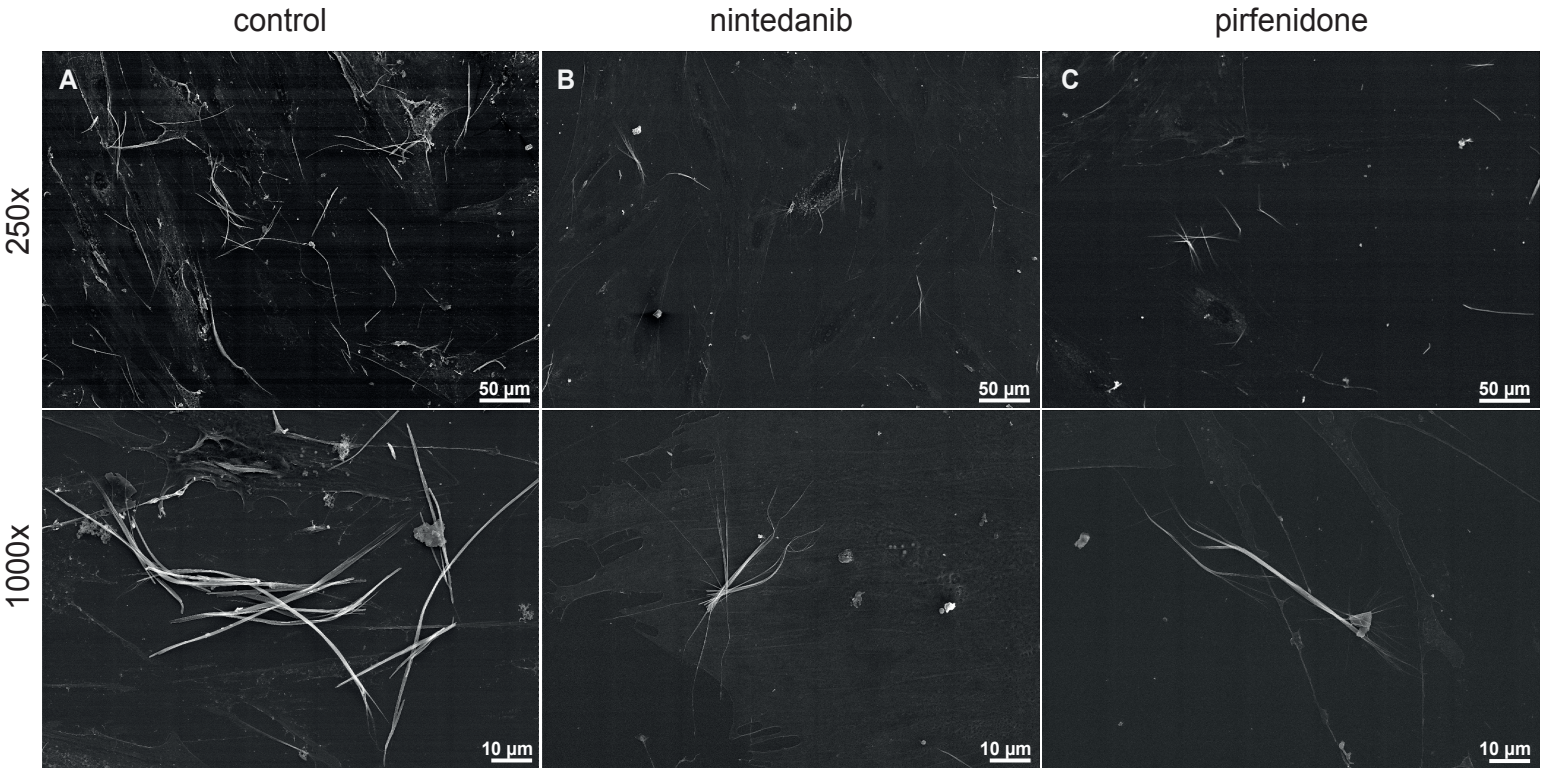

B

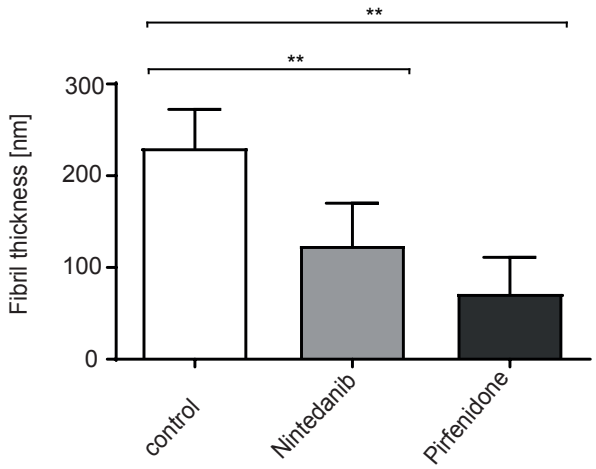

AJRCMB Articles in Press. Published on 03-March-2017 as 10.1165/rcmb.2016-0217OC

Figure 7

A

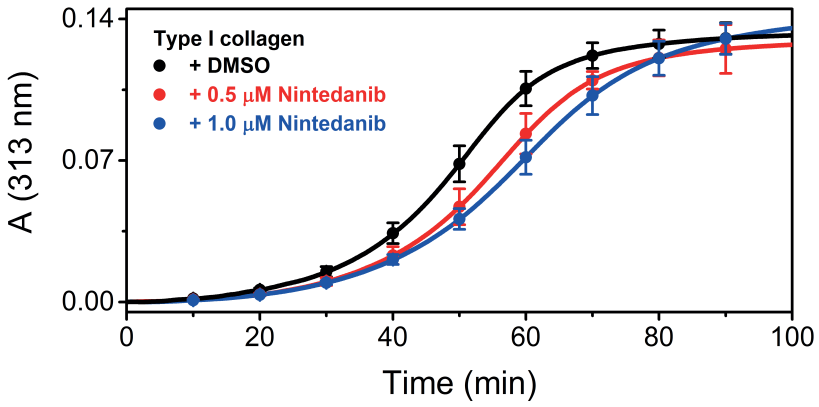

B

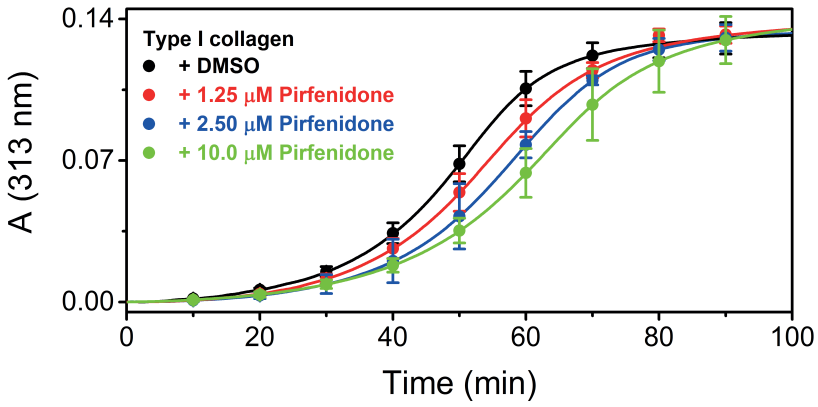

A NOVEL ANTIFIBROTIC MECHANISM OF NINTEDANIB AND PIRFENIDONE: INHIBITION OF COLLAGEN FIBRIL ASSEMBLY

Larissa Knüppel[1], Yoshihiro Ishikawa[2], Michaela Aichler[3], Katharina Heinzelmann[1], Rudolf Hatz[4,5], Jürgen Behr[5,6], Axel Walch[3], Hans Peter Bächinger[2], Oliver Eickelberg[1,7] and Claudia A. Staab-Weijnitz[1]

ONLINE DATA SUPPLEMENT

Material and Methods

Material:

Primers were purchased by MWG Eurofins (Ebersberg, Germany) and are listed in Supplementary Table E1. Used primary antibodies are given in Supplementary Table E2. Secondary HRP-linked antibodies were purchased from GE Healthcare Life Sciences (Freiburg, Germany).

Statistical analysis

Statistical analysis was performed in GraphPad Prism 7.02 (GraphPad Software, San Diego, CA). For quantification of transcript and protein, results are given as mean ± SEM of independent experiments with fibroblasts derived from at least four different IPF patients. Paired t-test was used for statistical analysis of fiber thickness and one way ANOVA (post test: Bonferroni`s multiple comparison test: comparison against control) was used for statistical analysis for all other experiments. Significance is indicated as follows: *$p<0.1$, **$p<0.01$, ***$p<0.001$, ****$p<0.0001$.

MTT Cytotoxicity Assay

To assess cytotoxicity of nintedanib and pirfenidone, 20.000 cells/cm^2 IPF fibroblasts were seeded in 24-well plates in absence and presence of TGF-β1 (R&D Systems, Minneapolis,

AJRCMB Articles in Press. Published on 03-March-2017 as 10.1165/rcmb.2016-0217OC

MN) (2ng/mL) in combination with nintedanib (0.01 μM, 0.1 μM, 1.0 μM) or pirfenidone (100 μM, 500 μM, 1000 μM) (both Selleck, Houston, TX) for 48h in starvation medium. Nintedanib and pirfenidone were dissolved in DMSO. The final DMSO concentration in the medium was always 1%.

After 48h thiazolyl-blue-tetrazolium-bromide (Sigma-Aldrich) in PBS was added to each well (final: 0.5mg/mL) and incubated at 37°C, 5% CO_2 for 30 min. The supernatant was aspirated and crystals were dissolved in 0.5 mL isopropanol/0.1% Triton X-100 for 30 min at room temperature on a shaker. Absorbance (570 nm) was measured using the Sunrise multiplate reader (Tecan; Männedorf, Switzerland).

Isolation and culture of primary human lung IPF and donor fibroblasts (phLF)

Lung specimens from IPF patients and healthy donors were dissected into pieces of 1-2 cm^2 followed by collagenase I (1 mg/mL) (Biochrom, Berlin, Germany) digestion at 37°C for 2 hours, filtration through nylon filters with a pore size of 70 μm (BD Falcon,Bedford, USA) and centrifugation at 400 *g* at 4°C for 5 minutes. Cells were resuspended in DMEM/F-12 medium (Life Technologies; Carlsbad, CA, USA) supplemented with 20% fetal bovine serum (Pan Biotech, Aidenbach, Germany) and penicillin/streptomycin (Life Technologies, Carlsbad, CA, USA) and seeded onto 10 cm cell culture dishes. For expansion, phLF were cultured in DMEM/F12 (Life Technologies) supplemented with 20% FBS (Pan Biotech) and penicillin/streptomycin (Life Technologies). Cells were routinely split when reaching a confluency of 80-90%. For this study, phLF from six different IPF patients were used in passages 5-8.

RNA isolation and Real-Time quantitative Reverse-Transcriptase PCR (qRT-PCR) Analysis

Isolation of RNA from cultured cells was performed by using the peqGOLD RNA isolation kit (Macherey-Nagel, Düren, Germany). Subsequently, RNA was reverse-transcribed

according to the manufacturer`s protocol (Life Technologies) in a 40 µL reaction using M-MLV reverse transcriptase and random hexamers. For quantitative real-time PCR (qRT-PCR) SYBR Green PCR master mix (Roche Applied Science, Mannheim, Germany) and primer mixtures given in Table 1 were used (95°C for 5 min, followed by 45 cycles of 95°C for 5 sec, 59°C for 5 sec and 72°C for 10 sec). Relative transcript abundance of a gene is expressed as -ΔCp values ($-\Delta Cp = Cp^{reference} - Cp^{target}$) or as Fold Change derived from the relevant ΔΔCp values, using $2^{-(\Delta\Delta Cp)}$. As endogenous control, DHX8 was used for standardization of relative mRNA expression.

Protein Isolation and Western Blot Analysis

To extract proteins from cultured cells, cells were scraped into Radio-Immunoprecipitation Assay (RIPA) buffer (50 mM Tris HCl pH 7.4, 150 mM NaCl, 1% Triton X100, 0.5% sodium deoxycholate, 1 mM EDTA, 0.1% SDS) containing a protease inhibitor and a phosphatase inhibitor cocktail (both Roche), incubated and centrifuged for 15 min at 13.000 rpm at 4°C. The supernatant was used to determine protein concentration via Pierce BCA Protein Assay (Thermo Fisher Scientific, Waltham, USA). After denaturation of the samples with Laemmli buffer (65 mM Tris-HCl pH 6.8, 10% glycerol, 2% SDS, 0.01% bromophenolblue, 100 mM DTT), proteins were resolved by SDS-PAGE and transferred to polyvinylidene difluoride (PVDF) membranes. The membrane was blocked for 1 hour at room temperature with 5% milk in TBS-T (0.1% Tween 20, TBS) to prevent nonspecific binding. Then, the membrane was shortly rinsed and washed (three times for 5 min) in TBS-T followed by incubation with primary antibody (Table 2) overnight at 4°C. After washing (three times for 5 min) and incubation with the secondary antibody for 1 hour at room temperature, the proteins were visualized with either SuperSignal™ West Dura Extended Duration Substrate or SuperSignal™ West Femto Maximum Sensitivity Substrate (both Thermo Fisher Scientific)

AJRCMB Articles in Press. Published on 03-March-2017 as 10.1165/rcmb.2016-0217OC

and analyzed by the ChemiDocXRS+ imaging system (Bio-Rad, Munich, Germany). Band quantification was performed in Image Lab (version 3.0, Bio-Rad, Hercules, CA).

Quantification of secreted collagen

Precipitation of collagen I and III was carried out as follows: 0.2 g/mL solid $(NH_4)_2SO_4$ was added to the supernatant and the solution was incubated on ice for 30 min. After centrifugation at 20.000 *g* for 30 min at 4°C, the pellet was dissolved in 1/10 of the original volume of 0.1 M acetic acid containing 0.1 mg/mL pepsin (Thermo Fisher Scientific) and incubated on ice overnight at 4°C. Subsequently, 5 M NaCl was added to a final concentration of 0.7 M, incubated on ice for 30 min followed by centrifugation at 20.000 g for 30 min at 4°C. The pellet containing collagen type I and III was resuspended in 0.1 M acetic acid and analyzed by Western blot.

Collagen precipitation for post-translational modification analysis

IPF fibroblasts were seeded at a density of 20.000 – 25.000 cells/cm^2 and cultured in DMEM/F12 (20% FBS, 0.1 mM 2-phospho-L-ascorbic acid, penicillin/streptomycin). When cells had reached a confluency of 80% serum-free DMEM/F12 medium (0.1 mM 2-phospho-L-ascorbic acid) was added containing TGF-β1 (2 ng/mL) and nintedanib (1 μM) or pirfenidone (1000 μM) or DMSO for control and incubated for 24h followed by collection of the medium. DMEM/F12 (20% FBS, 0.1 mM 2-phospho-L-ascorbic acid, penicillin/streptomycin) containing TGF-β1 (2 ng/mL) was added for 24h, followed by alternating cycles of serum-free media supplemented with TGF-β1 and nintedanib or pirfenidone or DMSO and media containing 20% FBS and TGF-β1. Serum-free cell culture supernatants were collected (20mL in each collection cycle) until 100 mL were obtained.

Precipitation of collagens from cell culture supernatant was in principle carried out in a scale-up version as described previously (1). 0.2 g/mL solid $(NH_4)_2SO_4$ was added to the supernatant and the solution was incubated on ice for 30 min. After centrifugation at 20.000 *g*

for 30 min at 4°C, the pellet was dissolved in 1/6 of the original volume of 0.1 M acetic acid containing 0.1 mg/mL pepsin (Thermo Fisher Scientific) and incubated on ice overnight at 4°C (Input). Subsequently, 5 M NaCl was added to a final concentration of 0.7 M, incubated on ice for 30 min followed by centrifugation at 20.000 g for 30 min at 4°C. After collection of the supernatant, the pellet was resuspended in 0.1 M acetic acid (0.7 M fraction). 5 M NaCl was added to the supernatant to a final concentration of 1.2 M and incubated on ice for 30 min, followed by centrifugation at 20.000 g for 30 min at 4°C. The supernatant was collected and the pellet was resuspended in 0.1 M acetic acid (1.2 M fraction). Again, 5 M NaCl was added to a final concentration of 2.5 M, incubated on ice for 30 min followed by centrifugation at 20.000 g for 30 min at 4°C. The pellet was resuspended in 0.1 M acetic acid (2.5 M fraction). The different fractions were resolved by SDS-PAGE (Input: 60 µL, 0.7 M fraction 20 µL, 1.2 M - 2.5 M fractions 80 µL) and visualized by Coomassie staining, followed by band excision, collagen digestion, mass spectrometry (MS) and amino acid analysis

Collagen Digestion and MS Analysis

SDS-PAGE bands were subjected to in-gel digestion with trypsin. Digest conditions were 13 ng/µl Promega trypsin in 100 mM ammonium bicarbonate at 37°C for 18h. Identification of tryptic peptides was performed on a Q-TOF Micro mass spectrometer (Waters, Billerica, MA) equipped with an electrospray ionization source. Data were collected with the MassLynx (version 4.1) data acquisition software (Waters) and processed using Mascot Distiller (Matrix Software, London, UK). High performance liquid chromatography was performed with a nanoACQUITY (Waters) system using a 75 µm x 100-mm 3-µm Atlantis dC18 column as the analytical column and a 180 µm x 20-mm 5-µm Symmetry C18 column as the trapping column. Chromatography mobile phases consisted of solvents A (0.1% formic acid and 99.9% water (v/v)) and B (0.1% formic acid and 99.9% acetonitrile (v/v)). Peptide samples were

AJRCMB Articles in Press. Published on 03-March-2017 as 10.1165/rcmb.2016-0217OC

loaded onto the trapping column and equilibrated for 2 min in 99% solvent A followed by a 120-min gradient to 60% solvent A at a constant flow rate of 1 µl/min. Analysis was performed in survey scan mode. Tryptic peptides were identified from MS/MS spectra by a Mascot search against the National Center for Biotechnology Information (NCBI) nr database (peptide tolerance 1.0 Da, MS/MS tolerance 1.0 Da)

Amino Acid Analysis

Acid Hydrolysis was performed in 6 x 50-mm Pyrex culture tubes placed in Pico Tag reaction vessels fitted with a sealable cap (Eldex Laboratories, Inc., Napa, CA). Samples were placed in culture tubes, dried in a SpeedVac (GMI, Inc. Albertsville, MN). Acid hydrolysis was performed in a reaction vessel that contained 500 µL of 6 M HCl (Pierce). The vessel was then purged with argon and the samples were hydrolyzed under vacuum at 110 °C for 24 h. The acid hydrolyzed samples were then dried under vacuum and reconstituted in 100 mL of 0.02 M HCl containing an internal standard (100 µM norvaline; Sigma). Analysis was performed by ion exchange chromatography with postcolumn ninhydrin derivatization and visible detection (440 nm/570 nm) with a Hitachi L-8800A amino acid analyzer (Hitachi High Technologies America, Inc., San Jose, CA) running the EZChrom Elite software (Scientific Software, Inc., Pleasanton, CA).

Base hydrolysis was performed in a reaction vessel that contained 100 µL of 4M NaOH per sample. The vessel was then purged with argon and the samples were allowed to hydrolyze under vacuum at 110 °C for 24 h. The base hydrolyzed samples were then dried under vacuum and reconstituted in 100 µL of 0.1M pH 9.5 borate buffer. 50 µL of 10 mM 4-fluoro-7-nitrobenzofurazan (NBD-F) in acetonitrile was added and the solution was incubated at room temperature for 6 hours. 100 µL of 0.2 M pH 2.0 tartarate buffer was added to the solution to quench the reaction. Analysis was performed by liquid chromatography on a 2695

HPLC (Waters, Inc. Milford, MA) with a Model 121 fluorometer detector (Ex. 460 Em. 530 Gilson Middleton, WI) running the MassLynx software

Collagen I fibril formation assay

A stock solution of collagen type I in 50 mM acetic acid was diluted to a final concentration of 0.1 μM into 0.1 M sodium bicarbonate buffer (pH 7.8) containing 0.15 M sodium chloride and 1 mM calcium chloride. Nintedanib (0.5 μM, 1 μM), pirfenidone (1.25 μM, 2.5 μM, 10 μM) or the same volume of DMSO (control) was added to the solution to obtain 0.5% final DMSO concentration. The solution was heated up to 34°C and the absorbance (light scattering) was recorded at 313 nm as a function of time.

Table E1. Primer table for qRT-PCR. Primers were synthesized by MWG Eurofins (Ebersberg, Germany).

Target	**Species**	**Forward primer** (5′-3′)	**Reverse primer** (5′-3′)
COL1A1	human	TACAGAACGGCCTCAGGTACCA	ACAGATCACGTGATCGCACAAC
COL3A1	human	ATCAACACCGATGAGATTAT	AGTATTCTCCACTCTTGAGTTC
COL5A1	human	CTTCAAGGTTTACTGCAAC	CCCTTCGGACTTCTTG
FN1	human	CCGACCAGAAGTTTGGGTTCT	CAATGCGGTACATGACCCCT
FKBP10	human	CGACACCAGCTACAGTAAG	TAATCTTCCTTCTCTCTCCA
SERPINH1	human	ATGTTCTTCAAGCCACAC	TCGTCGTCGTAGTAGTTGTA
PAI-1	human	GACATCCTGGAACTGCCCTA	GGTCATGTTGCCTTTCCAGT
DHX8	human	TGACCCAGAGAAGTGGGAGA	ATCTCAAGGTCCTCATCTTCTTCA

AJRCMB Articles in Press. Published on 03-March-2017 as 10.1165/rcmb.2016-0217OC

Table E2. Primary antibodies. Primary antibodies which were used for Western Blot analysis. Secondary HRP-linked antibodies were purchased from GE Healthcare Life Sciences (Freiburg, Germany).

Target	**Antibody**	**Provider**
ACTB	HRP-conjugated anti-ACTB antibody	Sigma Aldrich, Louis, MO, USA
AKT	rabbit polyclonal anti AKT antibody	Cell Signaling, Boston, USA
Collagen type I	rabbit polyclonal anti-Collagen I antibody	Rockland, Gilbertsville, PA, USA
Collagen type III	rabbit polyclonal anti-Collagen III antibody	Rockland, Gilbertsville, PA, USA
Collagen type V	rabbit polyclonal anti-Collagen V antibody	Santa Cruz, Dallas, TX, USA
ERK1	mouse monoclonal anti-ERK1 antibody	BD Biosciences, New Jersey, USA
Fibronectin	rabbit polyclonal anti-Fibronectin antibody	Santa Cruz, Dallas, TX, USA
FKBP10	rabbit polyclonal anti-FKBP10 antibody	ATLAS, Stockholm, Sweden
HSP47	mouse monoclonal anti-HSP47 antibody	Enzo Life Sciences, Inc., USA
p-AKT	rabbit monoclonal anti-pAKT (Ser473) antibody	Cell Signaling, Boston, USA
p-ERK	rabbit monoclonal anti-pERK1/2 (Thr202/Thr204)	Cell Signaling, Boston, USA

Figure E1: Effect of nintedanib and pirfenidone on the viability of phLF from IPF patients

Effect of increasing concentrations of nintedanib (0.01 μM, 0.1 μM, 1μM) and pirfenidone (100 μM, 500 μM, 1000 μM) on the viability of phLF of IPF patients after 48h treatment in combination with and without TGF-β1 (2 ng/mL), as measured by MTT assay. n=2.

Figure E2: Nintedanib reduces FN1 expression similarly in IPF and donor fibroblasts

(**A-D**) Quantitative reverse transcriptase-polymerase chain reaction analysis of phLF isolated from (**A, C)** IPF patients or (**B, D**) healthy donors treated for 48h with increasing concentrations of nintedanib (0.01, 0.1, 1 μM) or pirfenidone (100, 500, 1000 μM) in absence or presence of TGF-β1 (2 ng/mL). Transcript levels of FN1 are shown as -ΔCt values (**A, B**) as well as as transcript fold changes (**C, D**) to show the effect normalized to control. DEAH (Asp-Glu-Ala-His) Box Polypeptide 8 (DHX8) was used as endogenous control. Data are based on 7 (IPF) or 3 (donor) completely independent experiments and are given as mean ± SEM. Statistical significance between control and different concentrations of nintedanib or pirfenidone is indicated by horizontal brackets and asterisks for -ΔCt values and asterisks only for fold changes relative to 1.

(**E, F**) Western Blot analysis of phLF isolated from (**E**) IPF patients or (**F**) healthy donors treated for 48h with increasing concentrations of nintedanib (0.01, 0.1, 1 μM) or pirfenidone (100, 500, 1000 μM) in absence or presence of TGF-β1 (2 ng/mL). Densitometric analysis and representative blots show the effect of nintedanib and pirfenidone on FN1 protein expression relative to β-actin (ACTB). Data are based on 8 (IPF) or 3 (donor) completely independent experiments and are given as mean ± SEM. Statistical significance between control and different concentrations of nintedanib or pirfenidone is indicated by horizontal brackets and asterisks.

AJRCMB Articles in Press. Published on 03-March-2017 as 10.1165/rcmb.2016-0217OC

Statistical analysis was performed by One-Way ANOVA (post test: Bonferroni`s multiple comparison test: comparison against control). (*p<0.1, **p<0.01, ***p<0.001, ****p<0.0001). The well-known effect of TGF-β1 on these transcripts and proteins was significant, but is not specified in the interest of clarity. ctrl = control; TGF-β1 = transforming growth factor β1.

Figure E3: *PAI-1* transcripts are downregulated by nintedanib in IPF and donor fibroblasts

(**A-D**) Quantitative reverse transcriptase-polymerase chain reaction analysis of phLF isolated from (**A, C)** IPF patients or (**B, D**) healthy donors treated for 48h with increasing concentrations of nintedanib (0.01, 0.1, 1 μM) or pirfenidone (100, 500, 1000 μM) in absence or presence of TGF-β1 (2 ng/mL). Transcript levels of PAI1 are shown as -ΔCt values (**A, B**) as well as as transcript fold changes (**C, D**) to show the effect normalized to control. DEAH (Asp-Glu-Ala-His) Box Polypeptide 8 (DHX8) was used as endogenous control. Data are based on 7 (IPF) or 3 (donor) completely independent experiments and are given as mean ± SEM. Statistical significance between control and different concentrations of nintedanib or pirfenidone is indicated by horizontal brackets and asterisks for -ΔCt values and asterisks only for fold changes relative to 1. The well-known effect of TGF-β1 on these transcripts was significant, but is not specified in the interest of clarity. ctrl = control; TGF-β1 = transforming growth factor β1. Statistical analysis was performed by One-Way ANOVA (post test: Bonferroni`s multiple comparison test: comparison against control). (*p<0.1, **p<0.01, ***p<0.001, ****p<0.0001). The well-known effect of TGF-β1 on these transcripts and proteins was significant, but is not specified in the interest of clarity. ctrl = control; TGF-β1 = transforming growth factor β1.

Figure E4: Selected PTMs are neither affected by nintedanib nor by pirfenidone

SDS gel electrophoresis of different fractions of collagens precipitated out of 100 mL cell culture media of primary human IPF fibroblasts treated with nintedanib (1 μM) or pirfenidone (1000 μM) in combination with TGF-β1 (2 ng/mL) (A). SDS gel bands (indicated by red boxes) corresponding to the α1-chain of type I collagen (upper red boxes) and the α2-chain of type I collagen (lower red boxes) of the 0.7 M and the 1.2 M fraction were extracted and trypsin digested (A). MS/MS data of the A1 site (Pro-986) of α1-chain of type I (B), A3 site (Pro-707) of α1-chain of type I collagen (C), A3 site (Pro-707) of α2-chain of type I collagen (D) and glycosylation site of hydroxylysine (Lys-174) (E) of control, nintedanib- and pirfenidone-treated samples show no qualitative difference in intensity of prolyl-3-hydroxylation or glycosylation at these sites.

Figure E5: After 48 h, the RTK inhibitor nintedanib consistently inhibits PDGFR/AKT signaling in IPF and donor fibroblasts but not FGFR/ERK signaling

(**A-D**) Western Blot analysis of phLF isolated from (**A, C**) IPF patients or (**B, D**) healthy donors treated for 48h with increasing concentrations of nintedanib (0.01, 0.1, 1 μM) in absence or presence of TGF-β1 (2 ng/mL). (**A, B**) Densitometric analysis and representative blots show the effect of nintedanib and pirfenidone on AKT phosphorylation relative to total AKT levels. (**C, D**) Densitometric analysis and representative blots show the effect of nintedanib and pirfenidone on ERK phosphorylation relative to total ERK levels. Data are based on 8 (IPF) or 3 (donor) completely independent experiments and are given as mean ± SEM. Statistical significance between control and different concentrations of nintedanib or pirfenidone is indicated by horizontal brackets and asterisks. Statistical analysis was performed by One-Way ANOVA (post test: Bonferroni`s multiple comparison test: comparison against control). (*p<0.1, **p<0.01, ***p<0.001, ****p<0.0001).

AJRCMB Articles in Press. Published on 03-March-2017 as 10.1165/rcmb.2016-0217OC

REFERENCES

1. Staab-Weijnitz CA, Fernandez IE, Knüppel L, Maul J, Heinzelmann K, Juan-Guardela BM, Hennen E, Preissler G, Winter H, Neurohr C, Hatz R, Lindner M, Behr J, Kaminski N, Eickelberg O. FK506-Binding Protein 10, a Potential Novel Drug Target for Idiopathic Pulmonary Fibrosis. *Am J Respir Crit Care Med* 2015; 192: 455-467.

Figure S1

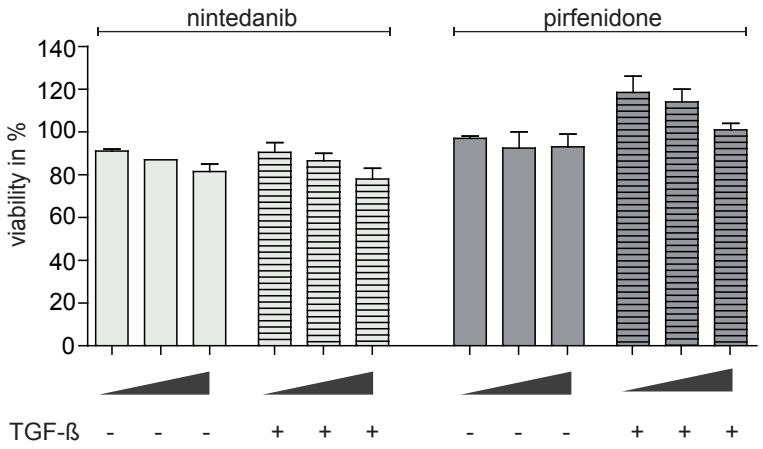

Figure S2 AJRCMB Articles in Press. Published on 03-March-2017 as 10.1165/rcmb.2016-0217OC

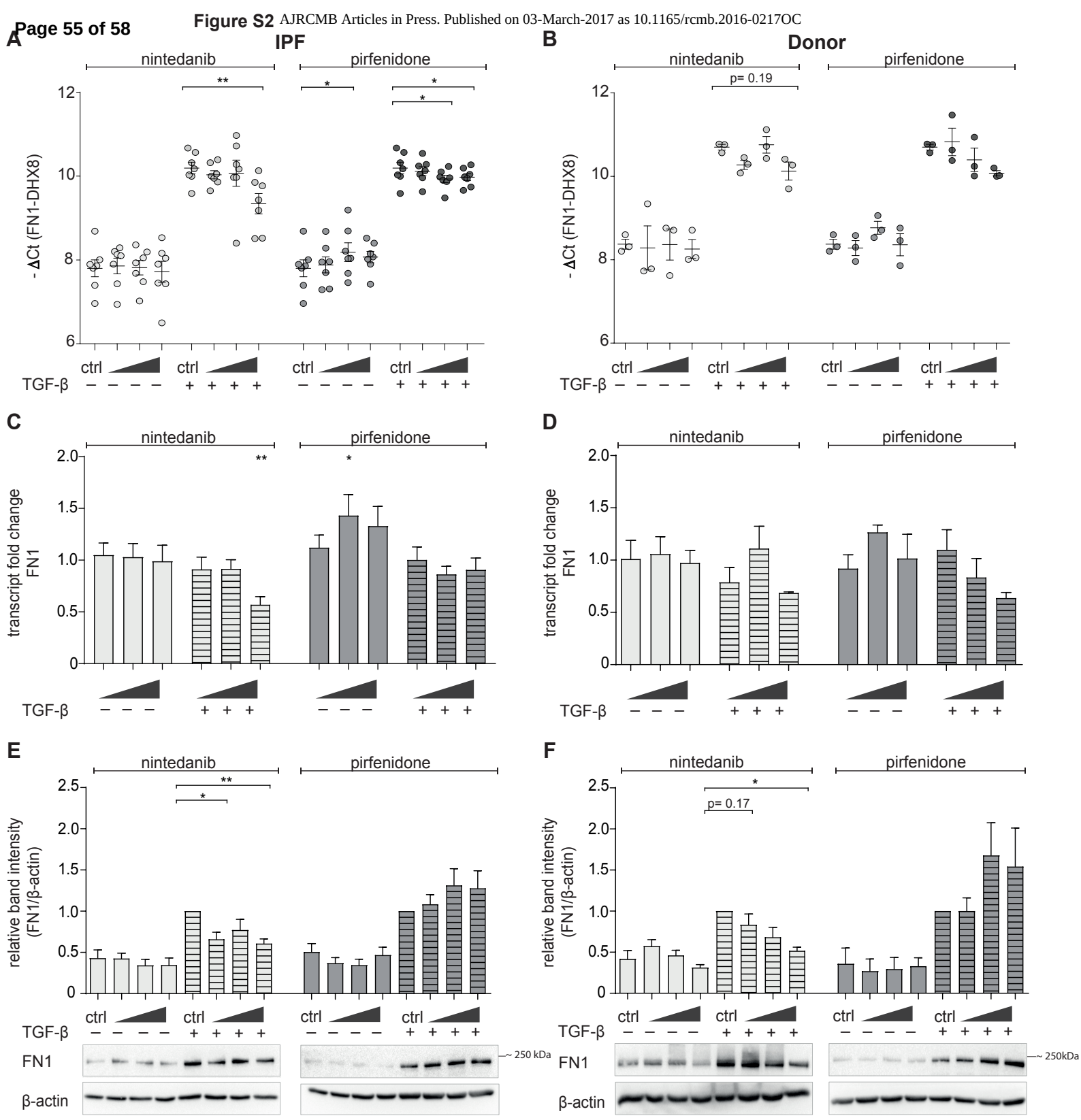

AJRCMB Articles in Press. Published on 03-March-2017 as 10.1165/rcmb.2016-0217OC

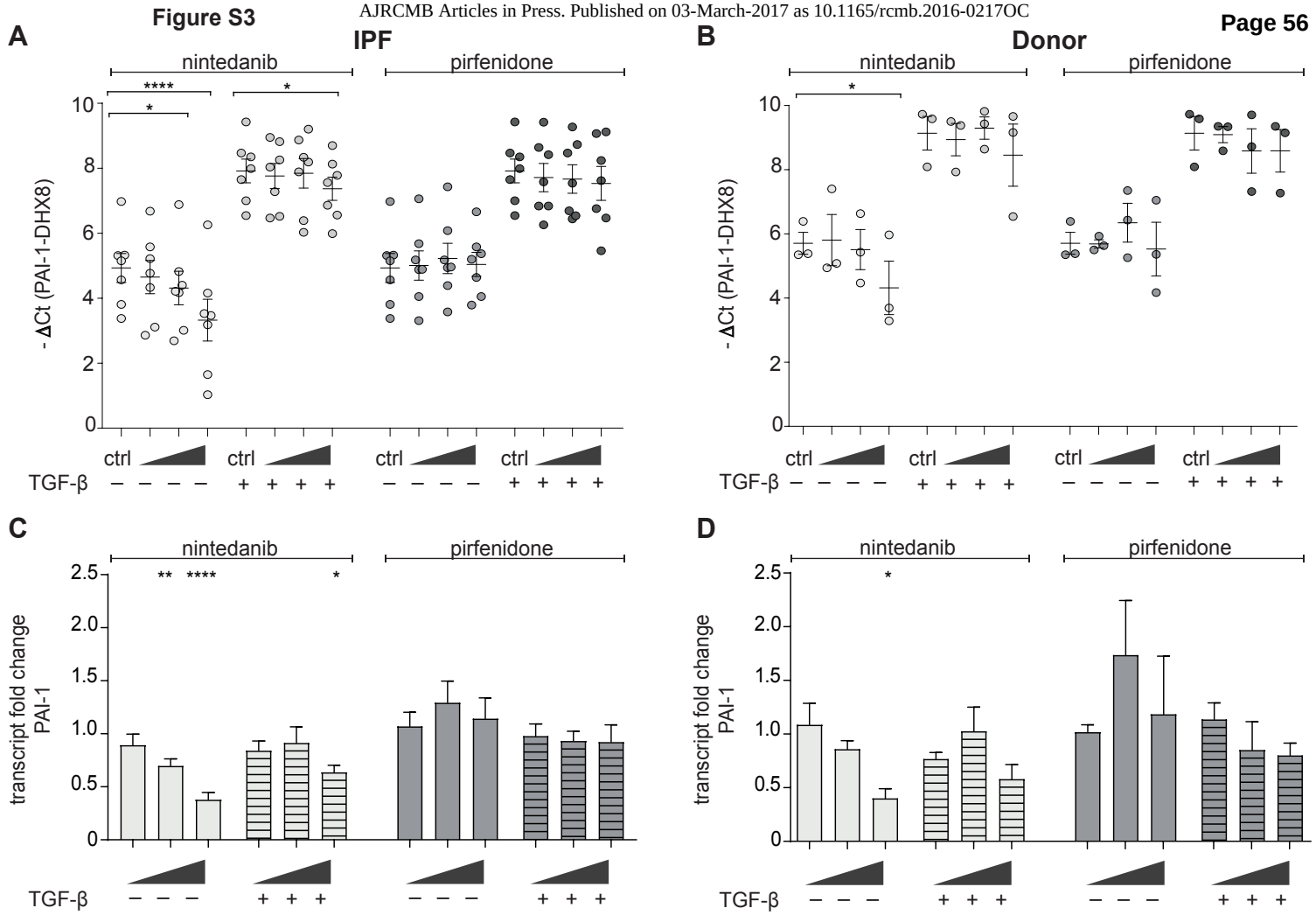

AJRCMB Articles in Press. Published on 03-March-2017 as 10.1165/rcmb.2016-0217OC

Figure S4

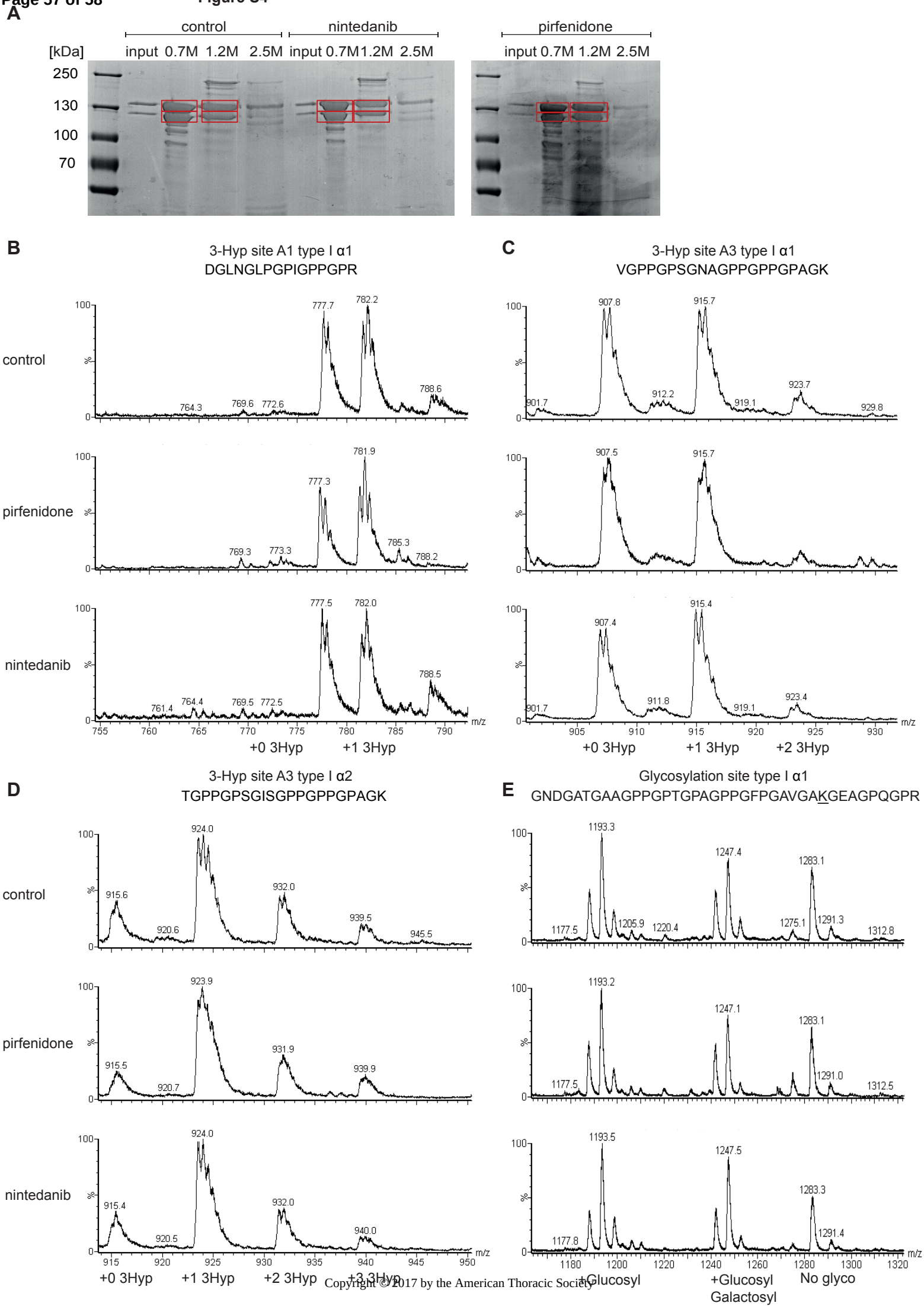

Figure S5